

# **URBAN TREE SPECIES CLASSIFICATION BASED ON SPECTRAL PROFILE OF CROWNS AND TEXTURE**

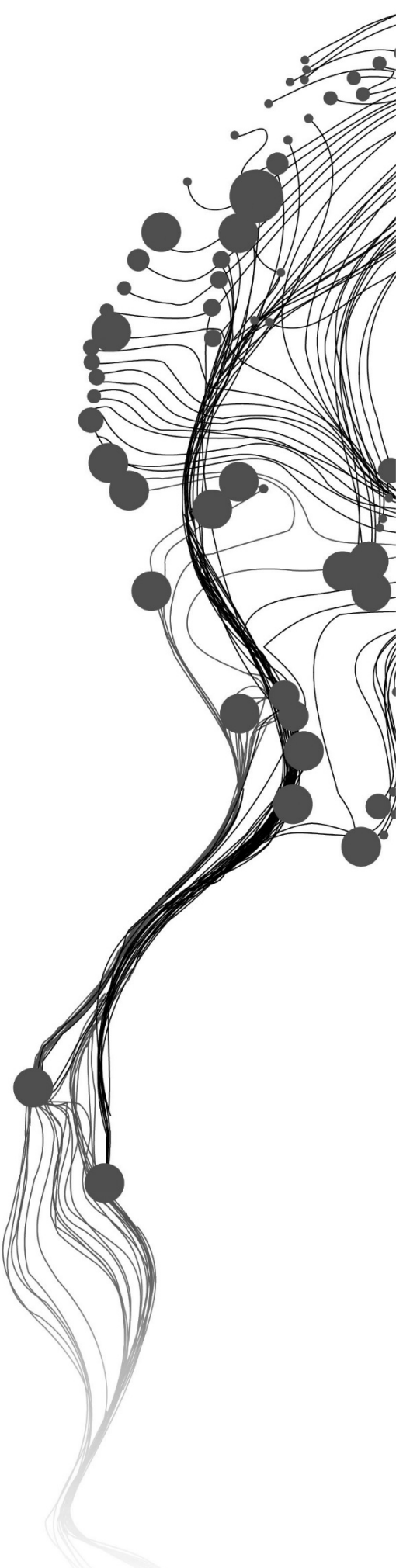
MAHBOOBEH RAMEZANI

March, 2015

SUPERVISORS:

Dr. Valentyn Tolpekin

Dr. Ir. Wietske Bijker

An abstract graphic on the left side of the page, resembling a tree or a complex network. It features a central vertical axis from which numerous thin, curved lines branch out. At the ends of these lines are various sized dark grey circles, some of which are larger and more prominent than others, suggesting nodes or data points. The overall shape is organic and flowing, extending from the bottom left towards the top right.

# **URBAN TREE SPECIES CLASSIFICATION BASED ON SPECTRAL PROFILE OF CROWNS AND TEXTURE**

**MAHBOOBEH RAMEZANI**

Enschede, The Netherlands, March, 2015

Thesis submitted to the Faculty of Geo-Information Science and Earth Observation of the University of Twente in partial fulfilment of the requirements for the degree of Master of Science in Geo-information Science and Earth Observation.

Specialization: Geoinformatics

**SUPERVISORS:**

Dr. Valentyn Tolpekin

Dr. Ir. Wietske Bijker

**THESIS ASSESSMENT BOARD:**

Prof.Dr.Ir. A. Stein (Chair)

Dr.Ir. B. G.H. Gorte (External Examiner, Delft University of Technology)

#### DISCLAIMER

This document describes work undertaken as part of a programme of study at the Faculty of Geo-Information Science and Earth Observation of the University of Twente. All views and opinions expressed therein remain the sole responsibility of the author, and do not necessarily represent those of the Faculty.

## ABSTRACT

Trees comprise a critical component of urban ecosystem and directly affect human habitation. Information on tree species is important for authorities, urban managers, landscape architects and environmentalists. Traditionally, identification of tree species is conducted through field based survey and visual interpretation of aerial photographs which are time consuming, costly and limited. In recent years, sensors have been launched and very high resolution imageries have become available which provide fast acquisition of information over a large area. However, using high resolution imagery for identification of tree species is a challenging issue due to increase of within class spectral variation by increase of resolution and low class separability between tree species and other urban vegetation. This research investigates the classification of urban tree species using spectral profile of tree crowns and texture.

In this research, the spectral profile is defined as the series of values of pixels along a transect polyline, if one applies the spectral profile for all pixels within the tree crown on an individual band of image, the result would be a surface. According to the research done by Ardila et al. (2012a) some tree species show different profiles across their crowns which is the hypothesis for this work. However, spectral profile does not perfectly fit a model because of the texture effect. Actually both effects of texture and spectral profile surface exist simultaneously (mixed effect). This poses a problem for texture analysis because texture analysis is affected by low frequency signal component.

In this research, coarse structure or low frequency signal component of tree crowns is described by bell curve models like Pollock, Gaussian and Paraboloid models. RMSE as a goodness of fit shows that the Pollock model can best approximate the coarse structure of tree crowns for all four species (*Plantanus Spp.*, *Corylus Spp.*, *Alnus Spp.*, and *Tilia Spp.*) compared to Gaussian and Paraboloid models. To describe the coarse structure of the trees of the same species just one model (the Pollock model) is sufficient. In addition, the difference between the coarse structures (surface model) of different tree species is defined by Pollock parameters which describe the shape of the spectral profile. It is observed that the geometrical shape of the tree crowns matches the shape of the spectral profile. In this regard, *Corylus Spp.* is completely separable from other species and *Alnus Spp.* and *Tilia Spp.* have the lowest class separability.

Fine structure or high frequency signal component is extracted by subtraction of the Pollock model from the spectral profile. In other words, the effects of texture and spectral profile surface are decomposed by subtraction of the fitted Pollock model from the spectral profile. GLCM texture measurements and semi-variogram are used for classification of fine structure. Addition of texture information for classification improves Kappa from 0.53 to 0.56 by considering the semivariogram and from 0.53 to 0.55 by considering GLCM texture measurements for classification. However, this improvement is not significant. Fine structure obtained from subtraction of the Pollock model from the spectral profile reveals more texture compared to the spectral profile itself. Classification based on texture of fine structure instead of texture of spectral profile has improved Kappa coefficient from 0.14 to 0.19. However, this improvement is not significant.

By applying Maximum likelihood classification based on both Pollock parameters and object-wise GLCM texture measurements, *Corylus Spp.* and *Plantanus Spp.* with conditional Kappa of 1.00 and 0.90 respectively classified almost perfectly. *Tilia Spp.* with conditional Kappa of 0.57 classified moderately and *Alnus Spp.* with conditional Kappa of 0.36 classified fairly. Although this research has been conducted in Delft city, the Netherlands, classification methods introduced in this research have this possibilities to be applied in other urban areas and to other species.

## ACKNOWLEDGEMENTS

My sincere thanks to the Netherlands Government through Netherlands Fellowship Programme (NFP) for sponsoring my studies at Faculty of Geo-Information Science and Earth Observation, University of Twente (ITC).

Foremost, I would like to express my sincere gratitude to my supervisors Dr. Valentyn Tolpekin and Dr. Ir. Wietske Bijker for the continuous support of my research, for their patience, motivation enthusiasm, and immense knowledge. Their guidance helped me in all the time of research and writing of this thesis.

Also, I would like to thank my fellow Geo-informatics classmates for classes we shared and for all the fun we had together. Last but not least, I would like to thank to my family for supporting me spiritually throughout my life.

# TABLE OF CONTENTS

---

List of figures .....	iv
List of tables .....	v
1. Introduction .....	7
1.1. Motivation and problem statement .....	7
1.2. Research identification .....	8
1.3. Research innovation aimed at .....	9
1.4. Method adopted .....	9
1.5. Thesis outline .....	10
2. Literature review .....	11
2.1. Tree species classification and remote sensing .....	11
2.2. Texture information for tree species classification .....	12
2.3. Shape information for tree species classification .....	12
2.4. Tree modeling .....	12
3. Concept and methodology .....	15
3.1. Spectral profile .....	16
3.2. Correction for the effect of geometry of sun illumination .....	17
3.3. Topographic normalization .....	18
3.3. Modeling the coarse structure of tree crowns .....	19
3.4. The fine structure of a tree crown .....	21
3.5. Textural descriptors based on Grey Level Co-occurrence Matrices (GLCM) .....	22
3.6. Variogram .....	24
3.7. GLCM texture measurements as a function of lag and window size .....	25
3.8. Texture measurements as the classification features .....	25
3.9. Classification and Accuracy assesment .....	26
4. Material and study area .....	29
4.1. Study area location: .....	29
4.2. Data .....	29
4.3. Software .....	30
5. Results .....	31
5.1. Fitting surface models to spectral profile of crowns .....	31
5.2. Maximum Likelihood Classification (MLC) based on Pollock parameters .....	34
5.3. Maximum Likelihood Classification (MLC) based on Pollock parameters and semivariogram model ...	36
5.4. Maximum Likelihood Classification (MLC) based on Pollock parameters and GLCM texture measurements .....	38
5.5. Classification based on GLCM texture measurements profiles .....	41
5.6. Summary of Classification .....	42
6. Discussion .....	43
6.1. Fitting surface models to spectral profile of crowns .....	43
6.2. Maximum Likelihood Classification (MLC) based on Pollock parameters .....	44
6.3. Maximum Likelihood Classification (MLC) based on Pollock parameters and texture measurements ...	45
7. conclusion and recommendations .....	49
7.1. Conclusion .....	49
7.2. Recommendations .....	49
List of references .....	51

## LIST OF FIGURES

---

Figure 1. NDVI profile of a tree crown .....	8
Figure 2. General framework of research.....	10
Figure 3. Methodology framework.....	15
Figure 4. Decomposition of a mixed signal to a high frequency and a low frequency signal component. ..	16
Figure 5. Lambert's Cosine Law .....	17
Figure 6. Lambertian surface .....	17
Figure 7. Geometry defining angle of incidence ( $\beta$ ) and solar zenith angle ( $\theta_s$ ) .....	18
Figure 8. Pollock surfaces with different values for $n$ .....	19
Figure 9. Obtaining fine structure by subtraction of the fitted surface model from the spectral profile .....	22
Figure 10. Obtaining fine structure by division of spectral profile by fitted Pollock model .....	22
Figure 11 Original spectral profile of a <i>Plantanus</i> crown, and fine structure of the same crown. ....	23
Figure 12. Obtaining GLCM matrix with different lags from the input image .....	23
Figure 13. Study area within Delft city.....	29
Figure 14. Changing accuracy (RMSE) by changing parameters $a$ , $b$ , and $n$ for fitting Pollock model. ....	32
Figure 15. Shape information for each tree species.....	33
Figure 16. Boxplots of Pollock parameters for each species.....	34
Figure 17. Extracting semi-variogram from fine structure of a crown and fitting a variogram model.....	36
Figure 18. Distribution of parameters extracted from fitted variogram model for each species. ....	37
Figure 19. GLCM measurements as a function of lag by applying a global (object-wise) window.....	38
Figure 20. Transformed divergence (TD) of GLCM texture measurements for each pair of species. ....	39
Figure 21. Mean and standard deviation of object-wise GLCM mean for each species. ....	41

## LIST OF TABLES

---

Table 1. Classification of Kappa coefficient. Source: Landis & Koch (1977) .....	27
Table 2. Characteristics of aerial image used for urban tree species classification.....	29
Table 3. Reference data used as training and verification sets. ....	30
Table 4. Root mean square error (RMSE) of fitting surface models to spectral profile of each species by applying two methods grid search and nonlinear regression.....	31
Table 5. Root mean square error (RMSE) as a goodness of fit of surface models.....	31
Table 6. Standards error of mean and confidence interval for mean of Pollock parameters.....	32
Table 7. Comparison of Kappa coefficient for two classifications, one based on parameters $a$ and $n$ as the descriptors and the other one by addition of parameter $b$ . ....	34
Table 8. Conditional Kappa coefficients for two classifications, one based on parameters $a$ and $n$ as descriptors and the other one by addition of parameter $b$ . ....	35
Table 9. Class separability (transformed divergence) between tree species based on Pollock parameters $a$ , $b$ and $n$ as descriptors .....	35
Table 10. Contingency analysis of training set based on Pollock parameters ( $a$ , $b$ , and $n$ ) .....	35
Table 11. Contingency analysis of verification set based on Pollock parameters ( $a$ , $b$ , and $n$ ).....	36
Table 12. Contingency analysis of the verification set based on the Pollock parameters and semi variogram model .....	37
Table 13. Comparison of Kappa coefficient for two classification, one based on Pollock parameters ( $a$ , $b$ and $n$ ) and the other one by addition of semivariogram parameters ( sill and range).....	37
Table 14. Correlation between texture measurements of for <i>Plantanus Spp.</i> ....	40
Table 15. Contingency analysis of classification base on the Pollock parameters and GLCM texture measurements computed from an object-wise window.....	40
Table 16. Contingency analysis of classification base on the Pollock parameters and GLCM texture measurements computed from pixel-wise window.....	41
Table 17. Comparison of Kappa coefficient for two classification, one based on object wise GLCM texture measurements of fine structure and the other one based on the object wise GLCM texture measurements of the spectral profile. ....	42
Table 18. Kappa coefficient for each classification and conditional Kappa for each species.....	42





# 1. INTRODUCTION

## 1.1. Motivation and problem statement

Trees are one component of urban infrastructure that play a significant role in improving air quality, energy conservation, recreation and urban hydrologic processes (Dwyer, Mcpherson, Schroeder, & Rowntree, 1992; Wolf, 2004, 2007). Information on tree species are important for environmentalists, urban managers, urban designers, and landscape architects. Authorities and urban managers need information on structure of urban vegetation for sustainable tree management to estimate the need for implementation of an urban forestry program, and to plan for a community's future. They need to incorporate species diversity when selecting a tree to plant. The loss of American elm from Dutch elm disease showed the danger of planting few species since these planting make the population prone to destruction from disease and pests (Endress, 1990). Moreover, choosing the right tree species in the right place is a prominent issue for urban designers and landscape architects, so they need to completely evaluate the site needs before selecting a tree species. In spite of great demand for accurate information about urban trees, recent studies (e.g., Brack, 2006) have shown that tree inventories are usually incomplete and need to be updated in most cities.

Satellite imageries are the alternative to traditional techniques for detection and monitoring of urban trees like field survey measurements, and visual interpretation of aerial photography. Being time consuming, prone to human errors, considerably expensive and limited to accessible areas, using traditional methods especially over a large area is not applicable. Moreover, because of rapid variation of urban landscape, having up to date information by using these techniques is a challenging issue (USDA, 2002). On the other hand, remote sensing methods provide timely effective and low cost information on urban vegetation. The main advantage of using remote sensing images is fast acquisition of information over large areas. Especially, with the advent of very of high resolution (VHR) images, the level of mapping in details have improved significantly (Thomas, Hendrix, & Congalton, 2003), but the needs for development of methods have been increased dramatically.

Although satellite imagery is an alternative data source for identification and classification of trees, there are some constraining factors. Trees in urban areas are difficult to extract due to limited spatial resolution of satellite images with respect to size of tree crowns. Recently numerous high resolution sensors have become available. However, the improvement of spatial resolution does not increase classification accuracy when pixel-based classification methods are used. There are some factors limiting the applicability of pixel based classifiers for tree species identification: (1) the increase of within class spectral variance with increasing resolution (Pouliot et al., 2002; Hirschmugl et al., 2007); (2) low spectral separability between tree species (Chepkochei, 2014) and other urban vegetation (Ardila et al., 2012a).

To solve the limitation of pixel-based classification, object-based methods have been developed which allow to work with regions instead of individual pixels. To extract spatial objects from an image, segmentation methods are applied which divide an image into regions which correspond to different objects or part of objects. Using these methods allow to extract very small features like small individual trees. In addition, image objects offer a wide range of variables for image analysis like texture, shape, and contextual features (Blaschke & Strobl, 2001; Blaschke, 2004; Blaschke, 2010; Hay & Castilla, 2008) which can be used for urban trees classification (Moskal, Styers, & Halabisky, 2011).

Texture is a property that represent the spatial variability of pixels over a region. It usually refer to high frequency signal component and can be used in object based image analysis (Lucieer, 2004). Many texture analysis methods have been developed such as grey level co-occurrence matrix (GLCM) (Haralick, et al., 1973), multivariate Gaussian Markov random field (Hazel, 2000), and local binary pattern (Ojala, Pietikainen, & Maenpaa, 2002). However, finding the reliable texture measurement and appropriate scale for tree classification especially in urban areas is a challenging issue.

Spectral profile is another property that shows the reflectance characteristic and distribution of pixel values inside tree crown objects and can perhaps be used for tree species classification. Spectral profile is defined as the series of values of pixels along a transect polyline. It is also defined as the value of one pixel in different bands of an image. According to the first definition, if we apply the spectral profile for all pixels within the tree crown on an individual band of image, the result would be a surface. Generally, tree crowns generate a bell-curve surface with local radiometric maxima near the centre of crown, which gradually decreases toward the crown boundary (Figure 1). Ardila et al. (2012a) fitted a Gaussian surface model to the NDVI radiometric surface of tree crowns to distinguish trees from other urban vegetation. According to their research, some tree species show different profiles across their crowns which is the hypothesis for this work. It is also important to consider that pectoral profiles may differ within a species according to age and also according to different varieties within species.

However, spectral profile does not perfectly fit a model because of the texture effect. Actually both effects of texture and crown profile surface exist simultaneously (mixed effect). This poses a problem for texture analysis because texture analysis is affected by low frequency signal component (Gross & Brajovic, 2003). This influence of the low frequency component can be a possible reason for failure of variance-based texture analysis of tree species in the research done by Chepkochei (2014). So decomposition of these two effect can be a hypothesis for this research.

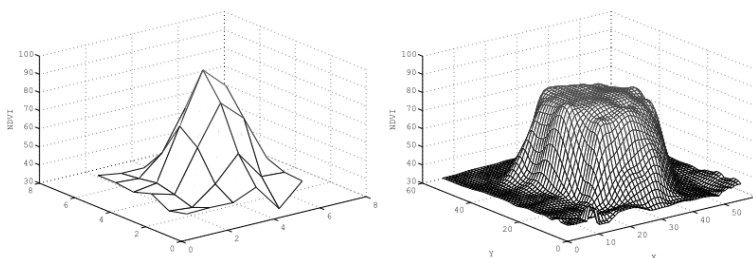


Figure 1. NDVI profile of a tree crown extracted from a Quickbird image with 2.4 m resolution and a VHR image with 0.25m resolution- Source: Ardila et al. (2012a)

## 1.2. Research identification

This research focuses on classification of urban tree species by using spectral profile of tree crowns by means of very high resolution imageries in order to provide accurate information on urban trees for strategic planning and decision making. The objectives and questions to be answered by this research are:

### 1.2.1. Research objectives

Main objective

To develop and implement image analysis methods to classify urban tree species of detected tree crowns on the very high resolution image by using spectral profile across tree crown and texture of tree crown.

Sub objectives

1. To decompose texture and spectral profile effects in tree crown.

2. To determine the best fitting surface for the spectral profile of each tree species and define the differences between these surfaces.
3. To define the difference between the textures of different tree species by using texture measurements
4. To determine the accuracy of classification based on texture measurements and surface fitting of tree crown

#### **1.2.2. Research questions**

1. How can texture and spectral profile effects be decomposed?
2. Which surface model can best approximate the spectral profile characteristics of each tree species?
3. How well the difference between the surface models of different tree species can be identified?
4. Does a single model describe profile of trees of the same species or is more than one model needed?
5. Which texture measurement can be used for tree species classification?
6. How well the difference between textures of different tree species can be identified?
7. Which tree species can be successfully detected?

#### **1.3. Research innovation aimed at**

This research aims at assessing the applicability and accuracy of classification and extracting information about tree species. In this research, for the first time tree crown spectral profile specifications like shape and texture are analysed for classification. Texture analysis have been used before for differentiating of trees from other land cover classes (e.g., Zhang, 2001). However, to the best of my knowledge, they have never been used for classification of tree species so far. Moreover, shape analysis of tree crown spectral profile in three dimensions has never been used before for classification of tree species.

#### **1.4. Method adopted**

To reach the objectives and answer the research questions, the following steps are taken: pre-processing, generation of fitting surface, classification using fitting surface and texture measurements, accuracy assessment, and validation.

- 1) Pre-processing: in this step the preprocessing functions like geo-referencing, and masking will be applied. Then, a suitable subset for analysis and classification and another subset for verification will be selected.
- 2) Generation of fitting surface model: in this step by having the crown polygons and training samples of detected species in the study area, analysis on the surface of spectral profile will be applied. Different surface models will be tested and the best fitting surface model or models with the least residuals will be selected for each tree species.
- 3) Texture analysis of spectral profile: in this step, by subtracting the fitting surface model from the spectral profile of the tree crown, the texture of the spectral profile will be obtained. Then the spectral profile texture will be analyzed by using different texture measurements like grey level co-occurrence matrix (GLCM).
- 4) Class definition: this step refers to analysis of texture and profile per class. Then, to determine how distinct and separable different tree species are from each other class separability will be computed.
- 5) Classification based on the spectral profile and texture: after defining the classes, classification methods based on the spectral profile and texture will be developed.
- 6) Accuracy assessment: in this step by using the verification dataset, accuracy of classified crowns will be estimated by using thematic accuracy assessments like Kappa and confusion matrix and different types of error will be identified.

Figure 2 shows the general frame work of the research.

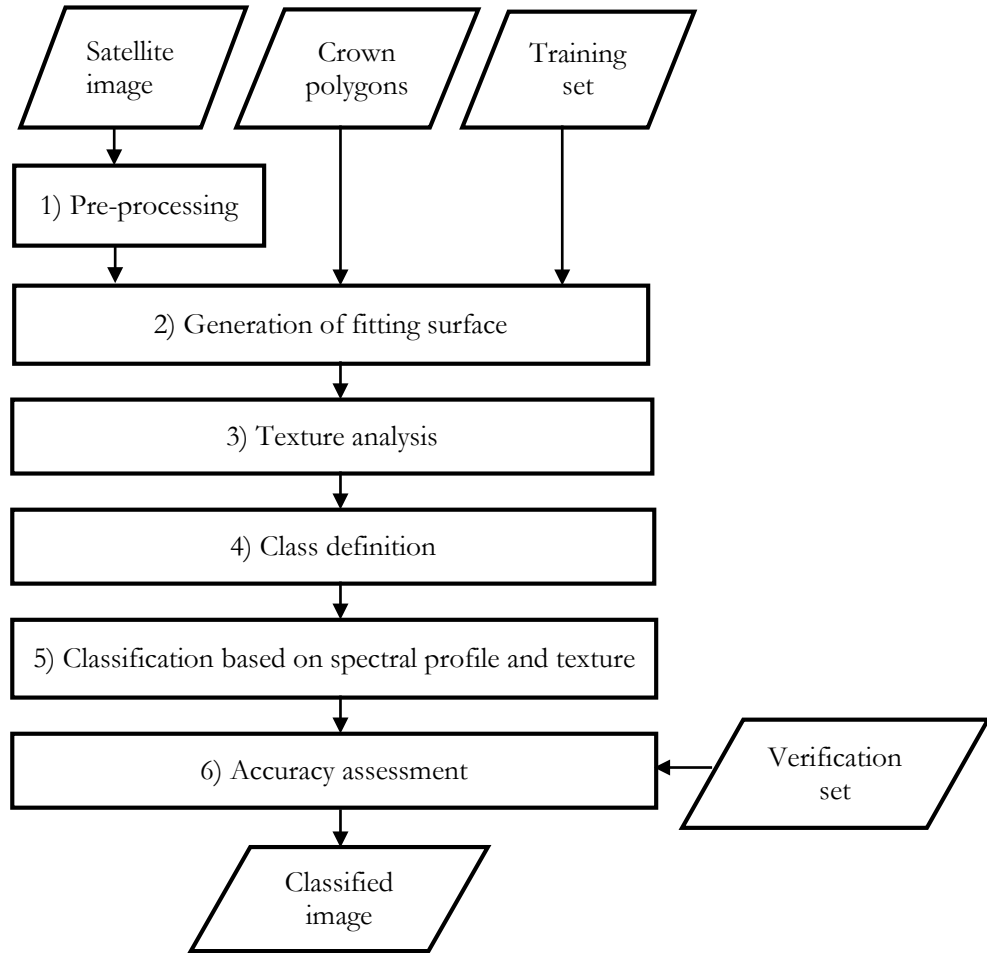


Figure 2. General framework of research

### 1.5. Thesis outline

This research is divided into seven chapters. The first chapter includes the problem statement, research objectives, research question, innovation that is aimed and general framework of research. The second chapter deals with literature review of the research regarding to tree modelling and texture measurements. The third chapter explains the concept and methodology applied in the research and chapter four introduces the study area, data and software used. Chapter five gives the results and chapter six deals with the analysis of results. The thesis ends with chapter seven which makes conclusion and recommendation for future researches in this area.

## 2. LITRATURE REVIEW

### 2.1. Tree species classification and remote sensing

Trees are an essential component of urban ecosystem that affect human life and urban environment. To identify tree species in urban areas, researchers have applied different methods. Since traditional techniques relying on interpreter's experience are not accurate enough, classification methods have been developed. These classification methods are based on the features, sometimes called descriptors (Brandtberg, 2002) or criteria (S. E. Franklin, Wulder, & Gerylo, 2001), which provide the highest separability between classes and highest within class similarity.

Tree species classification has benefited from advances in remote sensing. In recent years, imagery from a wide range of sensors have become available. This trend is likely to increase in the near future. However the choice of the most appropriate data source is a challenging issue and depends on some factors like the size of analysed objects, spatial resolution and extend of the available images, and also spectral and temporal image characteristics (Key, Warner, McGraw, & Fajvan, 2001). Medium resolution sensors like Landsat TM, SPOT, IRS, MOS which have a spatial resolution from 20m to 60 m, have been used for identifying tree species (Roller, 2000). For example, WHITE et al. (1995) applied an unsupervised classification on Landsat TM for defining species composition of forests. They modified spectral classification by environmental data and identified four classes (genus Pinus, genus Abies, non-wooded, without vegetation) with 73 percent accuracy. At that time, classification accuracy was dependent on spectral resolution, spatial resolution and study sites.

Until 1999, before launching IKONOS-2, the spatial resolution of available satellite images was incompatible with the geometric precision and level of details for tree mapping (Carleer & Wolff, 2004). At that time, aerial photographs were a widely used data source for vegetation mapping. Meyera, Staenzb, & Ittena (1996) identified five tree species in forest of "Unterwald" in Switzerland by using scanned aerial photographs. The advent of high spatial resolution sensors like IKONOS and QuickBird provided a new possibility for tree mapping and image analysis. Several studies demonstrated the capacity of VHSR images for identification of tree species (e.g. Hájek, 2006; Mora et al., 2010; Pu & Landry, 2012). Zhang et al. (2008) combined airborne VHR optical and light detected and ranging (LIDAR) imagery for classification of tree species over a mixed conifer hardwood forest in Ontario, Canada. Pu & Landry (2012) explored the potential of newly developed high resolution satellite sensors WorldView-2 and IKONOS for mapping urban tree species in city of Tampa, FL, USA.

High spatial resolution sensors generally provide data with limited spectral and temporal resolution due to their small field of view (FOV). A number of studies tried to overcome this limitation by combining multi-temporal images of lower spatial resolution. For example Key et al. (2001) discriminate four deciduous tree species by using differences in spectral properties of multi-temporal images and phenologic events between tree species. Most tree classification studies have used spectral signature approaches like maximum likelihood classifier (Sugumaran et al., 2003; Carleer & Wolff, 2004; Hagner & Reese, 2007). Leckie (2003) developed spectral signature for five conifer classes and one deciduous broad leaf class to classify old growth conifer sites along the west coast of Canada and got average error of 7.25% over the 16 sites.

One of the challenges in using high spatial resolution imagery and traditional pixel based classifiers like maximum likelihood which apply spectral signature feature is the increase of within class spectral variation.

In this regard, new multispectral classification approaches have been developed where individual tree crown, rather than pixel are the object of classification (Gougeon, 1995; Key et al., 2001; Leckie, 2003; Chepkochei, 2014). For example in the research by Leckie (2003), after applying pixel based maximum likelihood classification, the class with the most frequently identified tree species was assigned to each crown. Also, In the research by Chepkochei (2014), after initial per pixel classification by SVM, each tree crown was labelled based on the highest total probability.

Segmentation and delineation of individual tree crowns has been an ongoing research field for many years (Erikson, 2004). Several object based methods have been developed to detect individual crown boundary automatically. The valley following approach (Gougeon & Leckie, 2003, Gougeon, 1995a), the local maxima (Wulder, Hall, Coops, & Franklin, 2004), texture grouping (Warner, Lee, & McGraw), and morphological operators (Barbezat & Jacot, 1999) are the popular ones. Ardila et al. (2012a) developed object based methods for identification of individual trees and tree groups in urban areas. In addition, (Ardila, Tolpekin, Bijker, & Stein (2011) applied Markov random field based super resolution mapping for delineation of urban trees and got 66 % accuracy. This method proved an improvement over other classification methods like maximum likelihood and support vector machine.

The review of literature shows the deficiency of existing classification method for identifying tree species due to low class separability between different tree species, and shows the need for improvement of methods.

## **2.2. Texture information for tree species classification**

Texture is a criteria for defining the characteristics of objects in vegetation and forestry application (S. E. Franklin et al., 2001). Several studies have demonstrated that texture analysis can improve spectral classification of high spatial resolution images (e.g. Franklin, Maudie, & Lavigne, 2001; Coburn & Roberts, 2004; Y. Zhang, 2001). Franklin et al. (2000) showed that addition of texture can make modest improvement in classification of mixed-wood forest stands in Alberta, Canada from 60% to 65%. Franklin, Wulder, & Gerylo (2001) applied first order (variance) and second order (spatial co-occurrence homogeneity) texture measurement methods to distinguish the forest classes from IKONOS imagery.

## **2.3. Shape information for tree species classification**

Since most of remote sensing studies on tree classification have been done in forest areas, shape information of trees is rarely used for classification in multispectral imagery (Fournier, Edwards, & Eldridge, 1995). Trees in forest area are more compact and experiencing more competition for resources. Consequently, in satellite images of forest area only a portion of the tree tops are visible. In contrast to forest trees, in urban area trees are more isolated and shape information are more specific (K. Zhang & Hu, 2012). Several studies used shape information to classify tree species. Zhang & Hu, (2012) used the longitudinal profiles of tree crown to classify six tree species. Kim & Hong, (2008) used crown shape parameters and canopy texture parameters to identify tree species in QuickBird imagery.

## **2.4. Tree modeling**

A general model for profile of a tree crown first was proposed by the botanist Henry Horn in one dimension (Horn, 1971). Pollock (1996) extend this model for two dimension and described, tree geometry by a generalized ellipsoid of revolution. A number of researches have used Pollock model as the basis for their work to delineate tree crowns (e.g. Larsen & Rudemo, 1997; Straub & Heipke, 2001; Gong, Sheng, & Blgling, 2002). Mayer et al. (1999) applied Pollock's model and investigated the suitability of DSM for classification of trees. By parameter estimation they differentiated coniferous and deciduous trees. Ardila et al. (2012c)

fitted a Gaussian function to the membership images of two date to differentiate the urban trees from other urban vegetation and to monitor crown changes. The review of literature reveals that Gaussian model is more suitable for describing deciduous trees regarding to its properties. Nevertheless, Pollock model, by having the shape parameter has proved its suitability for modelling both deciduous and coniferous trees. The Pollock model mostly has been applied on the height data like DSM and been used for delineation of tree crowns. However, the suitability of this model for application on radiometric data and classification of tree species has not been explored so far. In addition regarding to properties of Gaussian model, it is more suitable for modelling deciduous trees.





### 3. CONCEPT AND METHODOLOGY

This chapter explains the methods applied to achieve the objectives. The methodology framework is shown in figure 3.

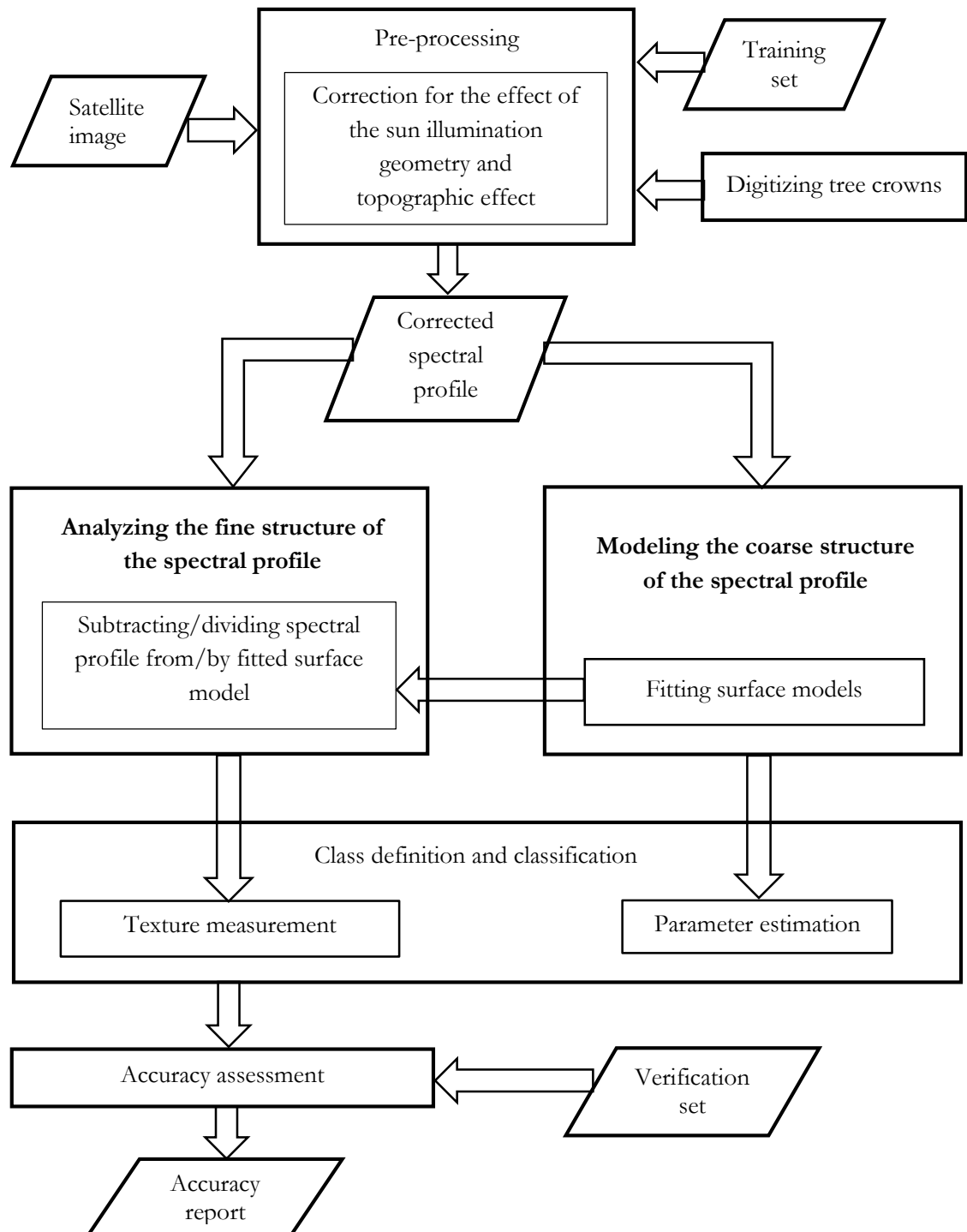


Figure 3. Methodology framework

### 3.1. Spectral profile

The spectral profile shows the reflectance characteristics of pixels inside a tree crown. In some software like ERDAS Imagine, spectral profile is defined as the value of one pixel in different bands of an image. In this thesis, a spectral profile is defined as the series of pixel values of an individual band along a transect polyline. In ERDAS Imagine, this is called a spatial profile. According to second definition, spectral profile of all pixels within a tree crown forms a bell shaped surface. From now on, wherever a spectral profile is mentioned, the second definition applies.

Two properties in the spectral profile of a tree crown which can be considered for analysis are as follows:

- 1) The bell curve shape of the spectral profile, in some literature called coarse structure (Wolf & Heipke, 2007) or low frequency signal component.
- 2) The detailed structure of the spectral profile, in some literature called fine structure (Wolf & Heipke, 2007) or high frequency signal component

In Figure 4, the green signal resembles the spectral profile of the tree crown that can be decomposed into two components, the high frequency signal component (yellow signal) and low frequency signal component (red signal).

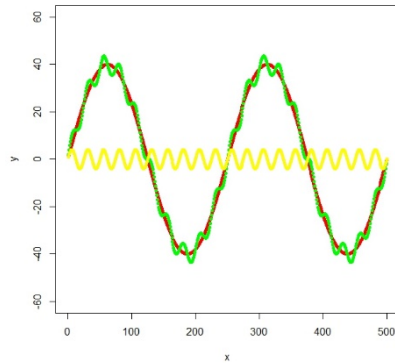


Figure 4. Decomposition of a mixed signal to a high frequency and a low frequency signal component. This figure shows a mixed signal (green signal) which can be decomposed into low frequency signal component (red signal), and high frequency signal component (yellow signal)

A decomposed profile allows analysis of separate components that can be useful for analysis. Therefore, two strategies can be taken as follows:

- 1) To model the coarse structure, or low frequency signal component, of the spectral profile by means of fitting a bell shaped surface model;
- 2) To analyze the fine structure, or high frequency signal component, of the spectral profile.

However, before retrieving the spectral profile, one needs to correct the effect of sun illumination geometry and topographic effect on each individual band of the image.

#### 3.1.1. Green-Red Vegetation Index (GRVI)

In this research, the spectral profile has been extracted from the Green-Red Vegetation Index (GRVI). GRVI can be computed as

$$GRVI = \frac{\rho_{green} - \rho_{red}}{\rho_{green} + \rho_{red}} \quad (1)$$

where  $\rho_{g.r.e.e.n}$  is reflectance of visible green and  $\rho_{r.e.d}$  is reflectance of visible red. In this research, the spectral profile has been extracted from GRVI instead of NDVI due to the limitation of available spectral bands. After this, “spectral profile” refers to spectral profile of a tree crown extracted from GRVI.

### 3.2. Correction for the effect of geometry of sun illumination

Correction of sun illumination is a necessary step of pre-processing in the remote sensing application. It is essential to determine the effect of geometry of illumination especially the solar zenith angle. Depending on the solar zenith angle, the sun illumination affects the spectral profile and may cause a shift in the profile curve and change the location of profile maxima. Therefore, images obtained from different solar zenith angles need to be corrected. To do so, tree crowns are assumed to be Lambertian surfaces and a cosine correction is applied. The solar zenith angle can be retrieved from the dataset or can be calculated on the basis of the exact date, time, and coordinates of the acquired image. In this research, within one image the solar zenith angle is assumed to be the same for entire image.

#### 3.2.1. Lambert's Cosine Law

Lambert's Cosine Law states that radiant intensity observed at a "Lambertian" surface is directly proportional to the cosine of the angle between the incoming light and the normal to the surface. As one can see in Figure 5, the irradiance falling on any surface varies as the cosine of the incident angle  $\theta$ . Accordingly, since at oblique angles the radiance spreads over a wider area, the irradiance is less than when that radiance is perpendicular to the surface. Lambert's Cosine Law can be written as

$$E_{\theta} = E \cos \theta \quad (2)$$

where  $E_{\theta}$  is the irradiance along a direction which has angle  $\theta$  with the normal to the surface,  $E$  is irradiance in normal direction,  $\theta$  and is the angle of incidence which is the angle between the illuminating source and the normal to the surface.

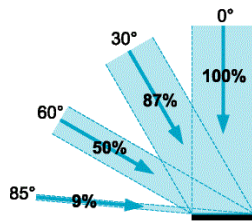


Figure 5. Lambert's Cosine Law Source: Ryer (1998)

In Equation 1, the assumption is that the reflecting surface is horizontal and Lambertian. A Lambertian surface provides a uniform diffusion of the incident radiation such that its radiation in all directions is the same. Accordingly, the reflected intensity is independent of the viewing direction, but dependent of the source orientation. Figure 6 shows a Lambertian surface. Since at  $60^\circ$  the radiance spreads over twice as large area, the reflection is half of the reflection at  $0^\circ$ .

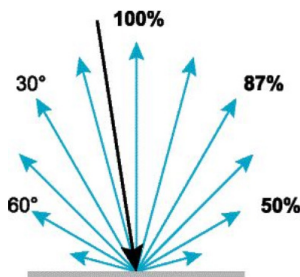


Figure 6. Lambertian surface Source: Ryer (1998)

### 3.2.2. Cosine correction for a horizontal surface

According to the Lambert's Cosine Law, the radiance observed by a sensor over a horizontal surface can be written as:

$$E_H = E \cos \theta_s \quad (3)$$

where  $E_H$  is irradiance on a horizontal surface at sensor,  $\theta_s$  is solar zenith angle, and  $E$  is irradiance in normal direction.

### 3.3. Topographic normalization

Measured spectral radiances are also subject to radiometric variations according to the slope and aspect characteristic of imaged tree crowns, just as they are subject to the effect of varying atmospheric and illumination conditions (Teillet, Guindon, & Goodenough, 1982).

#### 3.3.1. Cosine correction for a sloping surface

Accordingly, for a sloping surface the radiance observed by a sensor can be written as:

$$E_T = E \cos \delta \quad (4)$$

where  $E_T$  is irradiance on a tilted surface, and  $\delta$  is the incident angle with respect to normal of tilted surface. According to Figure 7, the measured spectral radiance at sensor may vary according to the slope and aspect of the imaged surface. Therefore, to eliminate measurement errors which may result from terrain topography and remove the effect of sloping surface, one can combine Equation 2 and 3 as

$$E_H = E_T \frac{\cos \theta_s}{\cos \delta} \quad (5)$$

where  $E_H$  is the irradiance on horizontal surface (normal reflectance),  $\theta_s$  is solar zenith angle.

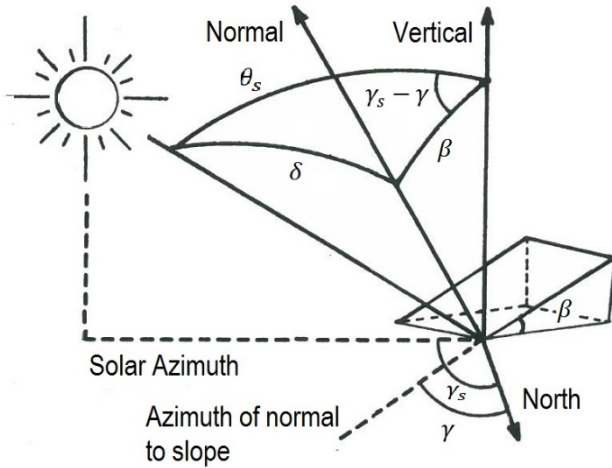


Figure 7. Geometry defining angle of incidence ( $\delta$ ) and solar zenith angle ( $\theta_s$ ) in case of a sloped surface  
Source: Teillet et al. (1982)

According to Figure 7, the angle  $\delta$  can be computed as

$$\cos \delta = \cos \beta \cos \theta_s + \sin \beta \sin \theta_s \cos(\gamma_s - \gamma) \quad (6)$$

Where  $\beta$  is slope angle,  $\gamma_s$  is the solar azimuth angle, and  $\gamma$  is the aspect of the slope.

#### 3.3.2. C-Correction

Teillet et al. (1982) proposed to emulate the effect of indirect illumination from the sky by adding a moderator ( $C$ ) to the cosine correction. A linear relationship exists between  $E_T$  and  $\cos \delta$  and one can model this relationship as

$$E_T = d + \beta \cos \delta \quad (7)$$

where  $\beta$  is the slope and  $d$  is the intercept of a linear regression between  $E_T$  and  $\cos \delta$ . Parameter  $C$  can be defined as a function of regression slope and intercept as follows

$$C = \frac{d}{\beta} \quad (8)$$

And exert a moderation to the cosine correction as

$$E_H = E_T \frac{\cos \theta_s + C}{\cos \delta + C} \quad (9)$$

### 3.3. Modeling the coarse structure of tree crowns

In this research, an assumption is made that geometric model of the tree crown surface can be applied to model the radiometric surface of the tree crown. This assumption is supported by visual inspection of radiometric surface of tree crowns in images. Three bell shaped surface models are considered, namely, Gaussian, Paraboloid, and Pollock models.

#### 3.3.1. Pollock model

Horn (1971) proposed a general model for one dimension vertical profile of a crown envelope (see equation 10). In the following equation,  $a$  and  $b$  are positive numbers and represent the vertical dimension (crown height) and horizontal dimension of a crown (crown radius), respectively, and  $n$  is positive and non-zero which represents the crown curvature.

$$\frac{z^n}{a^n} + \frac{y^n}{b^n} = 1 \quad (10)$$

When  $n = 1$ , the curve is a straight line. When  $0 < n < 1$ , the curve is upward concave and while  $n > 1$  is downward concave. When  $n = 2$  the curve is part of an ellipse.

Pollock (1994, 1996) extended Horn's model into two dimensions and defined a crown with a generalized ellipsoid. See the following equation.

$$\frac{z^n}{a^n} + \frac{(x^2 + y^2)^{\frac{n}{2}}}{b^n} = 1 \quad (11)$$

In this equation,  $x$  and  $y$  are the  $x$  and  $y$  coordinates and  $z$  is the height of tree crown for each location within tree crown. The intersection of model into the  $x$ - $y$  plane is a circle. Pollock surfaces with different values of  $n$  according to Equation 11 are shown in Figure 8.

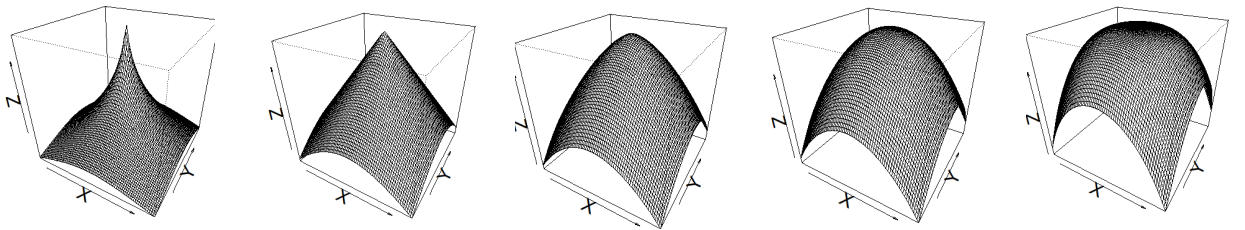


Figure 8. Pollock surfaces with different values for  $n$ . From left to right  $n$  equals 0.5, 1, 1.5, 2, and 3

As is shown in Figure 8, while  $n$  tends to zero the shape becomes more and more concave and tends to a disc shape with a spike along the  $z$  axis. When  $n = 1$  the shape tends to a cone. For  $n = 2$  the crown is a regular ellipsoid. For  $n > 2$  the model tends more and more to a cylinder (Larsen & Rudemo, 1997).Gong

et al. (2002) investigate a range of values for  $n$  from 1.0 to 1.8 with a typical value of 1.2 for coniferous trees and a range of values from 1.5 to 2.5 with a typical value of 2 for deciduous trees.

In the previous studies, Pollock model has been used to model the height information of the tree crowns whereas in this research it is used for modelling the spectral profile (the reflectance information). Consequently, for this study parameter  $a$  in Equation 10 and 11 represents the height of spectral profile, instead of the height of tree crown and  $z$  represents the reflectance value.

### 3.3.2. Isotropic and anisotropic Pollock model

Spectral profile of tree crowns can be modelled as an isotropic object with parameters computed by surface fitting of a Pollock model. By converting the Cartesian coordinates into polar coordinates Equation 10 can be written as follows

$$\frac{z^n}{a^n} + \frac{r^n}{b^n} = 1 \quad (12)$$

where  $r$  is the radius of tree crown and equals to  $\sqrt{x^2 + y^2}$ . The Pollock model can be extended to an anisotropic model in order to fit any elliptical tree object. The equation of an anisotropic Pollock model with rotated axes  $(x', y')$  fitted to GRVI values in the  $(x, y)$  locations of the image is

$$\frac{z^n}{a^n} + \left[ \left( \frac{x'}{b_x} \right)^2 + \left( \frac{y'}{b_y} \right)^2 \right]^{\frac{n}{2}} = 1 \quad (13)$$

Where  $b_x$  and  $b_y$  are width and length of an ellipse and the axes  $(x', y')$  rotated by an angle  $\alpha$  in counter-clockwise direction with respect to  $(x, y)$  are defined as:

$$x' = x \cos \alpha - y \sin \alpha \quad (14a)$$

$$y' = x \sin \alpha + y \cos \alpha \quad (14b)$$

### 3.3.3. Gaussian and Paraboloid as tree models

Other bell curve surface models that can be used for modelling spectral profile of tree crown are Gaussian and Paraboloid model. According to Equation 15, a Gaussian model can be defined by parameter  $h, \sigma_x, \sigma_y$ ; where  $h$  represents the height of Gaussian and  $\sigma = (\sigma_x, \sigma_y)$  represents the width of the elliptical Gaussian. In this equation,  $x'$  and  $y'$  are rotated  $x$  and  $y$ .

$$\text{Ga}(x, y) = h \exp \left[ -\frac{1}{2} \left( \left( \frac{x'}{\sigma_x} \right)^2 + \left( \frac{y'}{\sigma_y} \right)^2 \right) \right] \quad (15)$$

Here is the equation of an elliptic Paraboloid

$$\left( \frac{x}{\lambda_x} \right)^2 + \left( \frac{y}{\lambda_y} \right)^2 = -\frac{z}{i} \quad (16)$$

In this equation,  $\lambda_x, \lambda_y$  and  $i$  are positive numbers;  $\lambda = (\lambda_x, \lambda_y)$  represents the width of the elliptic Paraboloid. Paraboloid has a cross section of an ellipse and if  $\lambda_x = \lambda_y$  it will have a cross section of a circle.

### 3.3.4. Fitting Pollock model

Since in the Pollock model  $z$  is in power of  $n$ , fitting of the Pollock model to the spectral profile data is problematic. For fitting the Pollock model two methods nonlinear regression and grid search have been applied. In the grid search, as is obvious from its name, a grid is generated by knowing the possible ranges for  $a, b$  and  $n$ . Then for each point in the grid (for each defined combination of  $a, b$  and  $n$ ) the mean of square error (MSE) has been computed. For each pixel within tree crown, error is the difference between the estimated value computed from the Pollock model and the reflectance value. Then the point in the grid with the least mean squared error is selected as the best fitting point.

In the nonlinear regression method, by knowing a possible range of  $n$  a sequence of values is defined for  $n$ . For each  $n$  in the sequence,  $z$  is risen to the power of this initial  $n$ . Then, by applying nonlinear regression  $a, b$  and  $n$  are estimated and the difference between the initial  $n$  and estimated  $n$  is calculated. Then the initial  $n$ , with the least absolute difference is chosen.

### 3.3.5. Goodness of fit

Computation of goodness of fit helps to know how well each surface model fits the spectral profile. As one can see in Equation 17, in this research the root mean square error has been chosen to define the goodness of fit.

$$RMSE = \sqrt{\frac{1}{N} \sum_{i,j} (z'_{i,j} - z_{i,j})^2} \quad (17)$$

In Equation 17,  $z'$  is the estimated value by fitted surface model and  $z$  is the reflectance value in the  $i, j$  position. In addition,  $N$  represents the total number of pixels of a crown. For choose the best model and comparing the performance of different models in fitting the spectral profile, one can use the RMSE as a goodness of fit. The model with least RMSE is the best fit of the spectral profile.

### 3.3.6. Parameter estimation and confidence interval on mean of each parameter

The difference between coarse structures (surface model) of different tree species can be defined by estimated parameters. For example, for the Pollock model this difference can be defined by parameters  $a, b$ , and  $n$  for each species

Since the reference data set is a sample and is not an exhaustive survey across the study area, there is sampling variability. In this research, the standard error of mean ( $SE_m$ ) is computed to find the sampling variability in the estimate of mean ( $m$ ) for each parameter for each species. The standard error of mean can be computed as

$$SE_m = \frac{s}{\sqrt{n}}, \quad (18)$$

where  $n$  the sample is size and  $s$  is the estimated standard deviation. Since the standard deviation of population ( $\sigma$ ) is unknown and is estimated by  $s$ , there is some uncertainty in  $s$  which follows a  $t$  distribution. Then, the confidence interval (CI) is calculated as

$$CI = m \pm t s / \sqrt{n}. \quad (19)$$

### 3.3.7. Uncertainty of fit

To find the uncertainty of fit for each parameter, first a tolerance for RMSE should be determined. Then, by keeping constant two parameters and changing only the third parameter, the possible range for that changing parameter in that certain tolerance can be computed.

## 3.4. The fine structure of a tree crown

After fitting the surface model to the spectral profile, the fine structure component can be obtained by subtraction of the fitted surface model from the spectral profile or by division of the spectral profile by the fitted model. Figures 9 and 10 show the fine structures obtained from subtraction and division respectively.



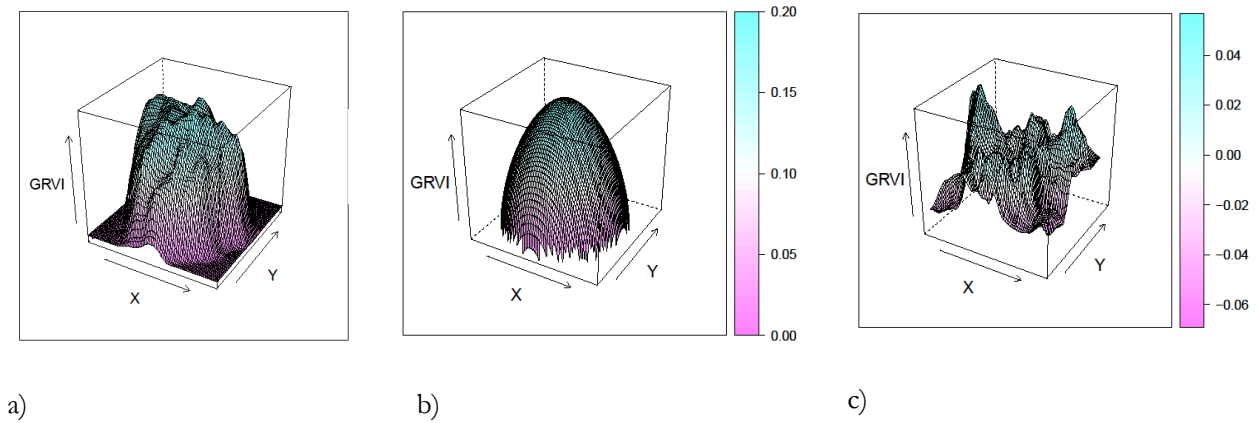


Figure 9. Obtaining fine structure by subtraction of the fitted surface model from the spectral profile; from left to right: spectral profile, fitted Pollock model, and fine structure of a tree crown

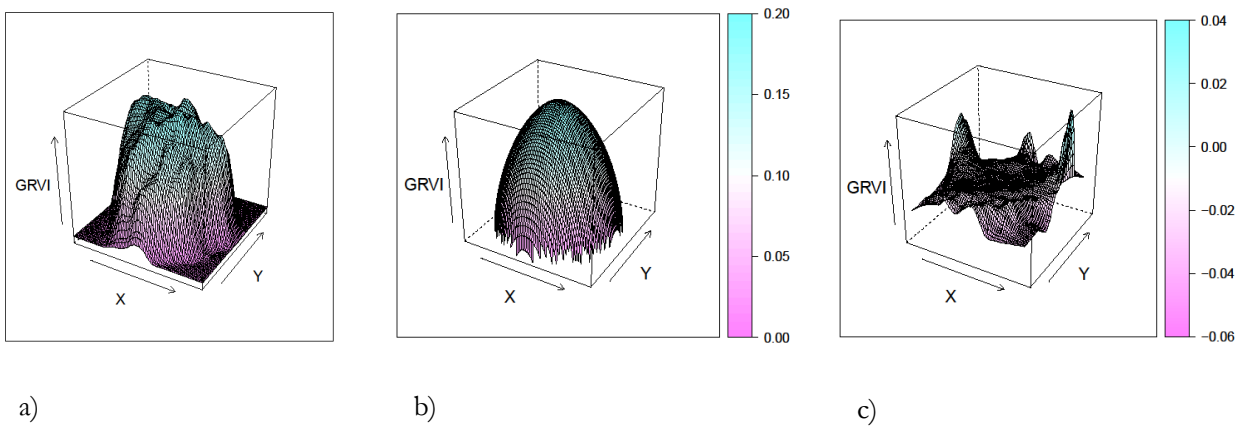


Figure 10. Obtaining fine structure by division of spectral profile by fitted Pollock model; from left to right: spectral profile, fitted Pollock model, and fine structure of a tree crown

As Figures 9 and 10 show, fine structure obtained from division is much smoother compared to the fine structure obtained from subtraction. By division procedure the mean of the residuals is close to zero and the standard deviation of the residuals is much smaller compared to the residuals obtained from subtraction. In fact, by division procedure there is no texture to be used for texture measurements. Therefore, the fine structure obtained from the subtraction procedure is used for further analysis and computing texture measurements. Furthermore, according to Figure 10, by division procedure the residuals close to the boundary are magnified because of division by a small number.

### 3.5. Textural descriptors based on Grey Level Co-occurrence Matrices (GLCM)

Difference in grey level values, scale of grey level differences, and directionality are the three variable that define a texture. One of the most widely used approaches to texture analysis is Grey Level Co-occurrence Matrix (GLCM) which was proposed by Haralick et al. (1973). They proposed a statistical method of examining texture by considering the spatial relationship of pixels in form of GLCM matrix. As one can see in Figure 11, by subtracting the fitted Pollock model from the spectral profile more texture is visible compared to the original spectral image.

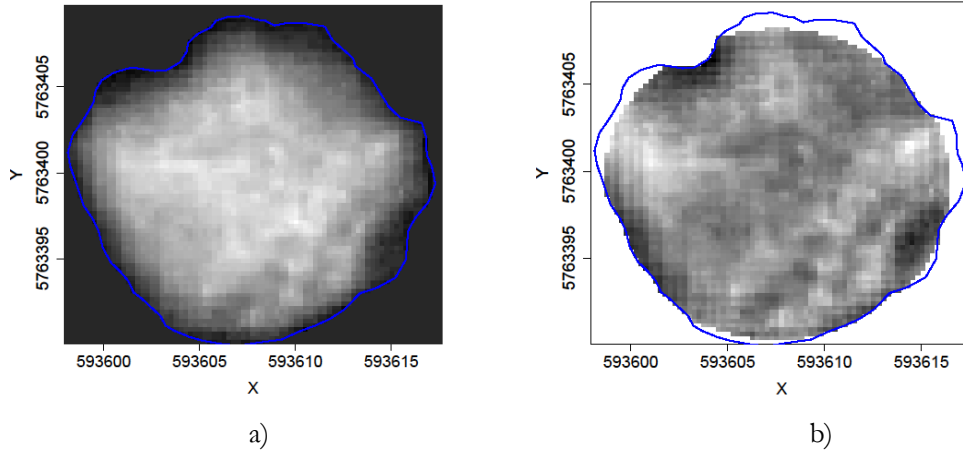


Figure 11 a) Original spectral profile of a *Plantanus* crown, b) fine structure of the same crown obtained from subtraction of the fitted Pollock model from the spectral profile.

### 3.5.1. Grey-Level Co-occurrence Matrix (GLCM)

GLCM define the texture of an image by computing how often different combinations of grey levels with different values and specified spatial relationship occur in an image. The number of grey levels in the image determines the size of the GLCM which can be reduced by quantization. A single GLCM might not be sufficient to define the textural characteristics of the input image. Pixel relationships can be defined by varying direction and distance. In texture analysis the distance between the reference pixel  $i$  and its neighbouring pixel  $j$  is described as lag or separation distance ( $h$ ). Note that here,  $i$  and  $j$  do not refer to pixel coordinates but pixel intensities. GLCM is computed over a specific number of neighbouring pixels which is defined as window ( $w$ ). In this research, the possible range of angle orientations are reduced to 4 angles of  $-45^\circ$ ,  $0^\circ$ ,  $45^\circ$ , and  $90^\circ$  and the effect of lag and window size on the texture of each tree species has been explored.

Figure 12 shows how the first element in a GLCM is computed in the direction  $0^\circ$  by different pixel separation distance. The element (1, 1) of GLCM matrix for the lag 1 pixel contains the value 2, since there are three pairs of pixels having value 1 in  $0^\circ$  direction in the input image. For the lag 2 pixels, this element of GLCM matrix contains the value 4 since there are 4 pairs of points having value 1 with separation of 2 pixels in direction  $0^\circ$  in the input image.

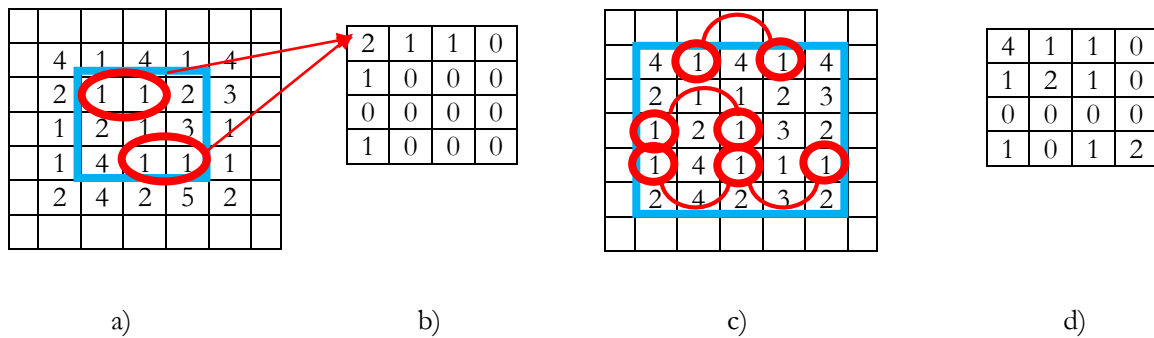


Figure 12. Obtaining GLCM matrix with different lags from the input image. a) input image, b) GLCM matrix with lag 1 pixel and window size 3 by 3 pixels in  $0^\circ$  direction, c) input image, d) GLCM matrix with lag 2 pixels and window size 3 by 3 pixels in  $0^\circ$  direction.

Several statistics can be derived from the GLCM matrix which provide information about the texture of an image. These statistics can be listed as follow (Haralick et al., 1973):

### 3.5.2. GLCM mean

$$\mu_i = \sum_{j=0}^{N-1} i (P_{i,j}), \quad \mu_j = \sum_{i=0}^{N-1} j (P_{i,j}) \quad (20)$$

where  $N$  is the number of grey levels and  $i, j$  are pixel intensities.

### 3.5.3. GLCM variance

$$\delta_i^2 = \sum_{j=0}^{N-1} P_{i,j} (i - \mu_i)^2, \quad \delta_j^2 = \sum_{i=0}^{N-1} P_{i,j} (j - \mu_j)^2 \quad (21)$$

### 3.5.4. GLCM contrast

GLCM contrast measures the local variations in the grey-level co-occurrence matrix. Contrast of zero in a vertical direction means that image has vertical stripes and contrast zero in all direction means an entirely uniform image. GLCM contrast can be computed as

$$\sum_{i,j=0}^{N-1} P_{i,j} (i - j)^2 \quad (22)$$

### 3.5.5. GLCM dissimilarity

GLCM dissimilarity is equivalent to the sum of absolute differences which can be computed as

$$\sum_{i,j=0}^{N-1} P_{i,j} |i - j| \quad (23)$$

### 3.5.6. GLCM homogeneity

GLCM homogeneity, also called inverse difference moment, measures the closeness of the distribution of elements in the GLCM to the GLCM diagonal which can be computed as

$$\sum_{i,j=0}^{N-1} \frac{P_{i,j}}{1+(i-j)^2} \quad (24)$$

### 3.5.7. GLCM angular second moment (ASM) and energy

GLCM angular second moment (ASM), also known as uniformity, provides the sum of squared elements in the GLCM. It can be computed as

$$\sum_{i,j=0}^{N-1} P_{i,j}^2 \quad (25)$$

Square root of the ASM is called energy and is used as a texture measure. High values of ASM and energy occur when the window is very orderly

### 3.5.8. GLCM entropy

GLCM entropy can be computed as

$$\sum_{i,j=0}^{N-1} P_{i,j} (-\ln P_{i,j}) \quad (26)$$

## 3.6. Variogram

Variogram also called semi-variogram,  $\gamma(h)$ , is used to represent and model the spatial variation of pixels which can be computed as (Webster & Oliver, 2008)

$$\gamma(h) = 0.5 E[Y(u) - Y(u+h)]^2 \quad (27a)$$

$$\gamma(h) = C(0) - C(h) \quad (27b)$$

In this equation,  $Y$  is a random function,  $u$  denotes location, and  $h$  is the distance between  $u_1$  and  $u_2$ .  $C(0)$  is sill which is the total variability denoted also as  $\sigma^2$  and  $C(h)$  is auto-covariance at lag  $h$  that can be computed as (Webster & Oliver, 2008)

$$C(h) = \text{Cov}[Y(u_1), Y(u_2)] = E[Y(u) Y(u+h)] - \mu_Y^2 \quad (28)$$

Variogram key parameters are range, sill and nugget. Range, denoted as  $\phi$ , is the distance (lag) up to which the regionalized variable is auto-correlated and is directly related to the size of textural features. Sill is the total variability and is proportional to the global variance of textural feature (Jakomulska & Clarke, 2000). The partial sill is computed by subtraction of nugget from the total sill a nugget is the non-spatial variability denoted as  $C_0$  or  $\tau^2$ . Cut off is the maximum lag up to which the sample variogram is estimated. In analysis usually the slope is computed by the division of the partial sill by the effective range. One should notice that the number of pairs of points used to estimate variogram should not be smaller than 30 and preferably should be larger than 45. In addition, one should check whether the variogram reaches a sill. If the sample variogram has not flattened out (i.e. reached the sill), then one should increase the cutoff and check whether the sill is reached at a longer lag. Sample variogram values tend to become erratic at long lags since at longer lags data tends to be less correlated and the number of pairs of points reduces at long lags which leads to unreliable estimates.

### 3.7. GLCM texture measurements as a function of lag and window size

Since GLCM texture measurement is a function of lag and windows size, for computing GLCM matrix following approaches have been taken:

1. GLCM with a pixel-wise window: In this approach for computing GLCM matrix a moving window has been considered and then for each texture measure, the lag and window size which provides the highest class separability have been chosen. In this approach, for each pixel inside the crown, there would be a GLCM matrix and a corresponding value for each GLCM texture measurement.
2. Global GLCM or object-wise GLCM: In this approach, the GLCM matrix has been computing from all pixels inside a crown. Consequently, for each tree crown there is a single GLCM matrix and a single value for its corresponding texture measurement.

A difference between these two approaches is that for computing GLCM with pixel-wise window, depending on the window size, just a limited number of pixels are involved. However, for computing global GLCM, all pixels inside of a crown are involved.

Another difference is the margin effect which exists for the pixel-wise window. Considering the window size and the lag, for pixels near the crown boundary the GLCM matrix cannot be computed and the pixels information will be lost.

### 3.8. Texture measurements as the classification features

Texture measures can be used as the input layers. They can be used alone or with other features for supervised or unsupervised classification. The mean and range of each measure can be used for class definition. In this research, for supervised classification of tree species, by using texture three approaches can be applied:

1. To compute the average of a pixel-wise GLCM texture measure for all pixels within a crown; assign the average of the texture measure for the crown and classify the tree crown based on this value.

2. To compute the standard deviation of a pixel-wise GLCM texture measure for all pixels within a tree crown; assign the standard deviation of the texture measure for the crown and classify the tree crown based on it.
3. To compute a GLCM texture measurement (pixel-wise or object-wise) in different lag distance for a tree crown; get the corresponding profile and classify the tree crown based on this profiles.

### 3.9. Classification and Accuracy assesement

#### 3.9.1. Maximum likelihood classification

A maximum likelihood classification has been used to classify the crowns by considering Pollock and texture parameters as the classification features or bands. Maximum likelihood classifier is one of the most popular methods of classification in remote sensing, which usually assumes that each class is normally distributed .It calculates the probability that a given pixel belongs to a specific class. To do so, a Bayesian probability function is calculated based on mean and covariance of the training set. Then, each pixel is assigned to the class that has the highest probability. Accordingly,  $P(i|\omega)$  is the posterior probability of a pixel with vector  $\omega$  belonging to class  $i$ . The vector  $\omega$ , known as feature vector can be a pixel DN value or the mean of a pixel-wise GLCM texture measurement for a crown or any other classification feature.  $P(i|\omega)$  can be computed as

$$P(i|\omega) = \frac{P(\omega|i)P(i)}{P(\omega)} \quad (29)$$

Where  $P(\omega|i)$  is the conditional probability to observe  $\omega$  from class  $i$  or the probability density function,  $P(i)$  is the probability that class  $i$  occurs, and  $P(\omega)$  is the probability that  $\omega$  is observed.

An error matrix is an effective way to represent classification accuracy. The major diagonal of error matrix represents the properly classified tree crowns and the non-diagonal values of matrix show the omission and commission error. A commission error can be defined as including a tree crown into a species class when it does not belong to that class. An omission error is excluding a tree crown from the species class in which it truly does belong.

#### 3.9.2. Accuracy assessment

An error matrix with  $n$  samples and  $k$  categories in the remotely sensed classification (usually rows in error matrix) and  $k$  categories in the reference data (usually column in the error matrix) has  $k^2$  cells. Accordingly  $n_{ij}$  represents the number of samples classified into species class  $i$  in the remotely sensed data and species class  $j$  in the reference data set. Let  $n_{i+}$  be the number of samples classified into species class  $i$  in the remotely sensed classification and  $n_{+j}$  be the number of samples classified into species class  $j$  in the reference data set. Then overall accuracy can be computed as

$$\text{Overall accuracy} = \frac{\sum_{i=1}^k n_{ii}}{n} \quad (30)$$

Kappa coefficient can be computed as

$$K = \frac{n \sum_{i=1}^k n_{ii} - \sum_{i=1}^k n_{i+} n_{+i}}{n^2 - \sum_{i=1}^k n_{i+} n_{+i}} \quad (31)$$

The test statistic for testing if two error matrices are significantly different is as follows (Russell & Kass, 1999)

$$Z = \frac{|K_1 - K_2|}{\sqrt{\text{var}(K_1) + \text{var}(K_2)}} \quad (32)$$

In Equation 31,  $K_1$  and  $K_2$  denote the estimated Kappa for error matrix 1 and 2 respectively.  $\text{var}(K_1)$  and  $\text{var}(K_2)$  are the corresponding estimates of the variance which can be computed as

$$\text{var}(K) = \frac{1}{n} \left\{ \frac{\theta_1(1-\theta_1)}{(1-\theta_2)^2} + \frac{2(1-\theta_1)(2\theta_1\theta_2-\theta_3)}{(1-\theta_2)^3} + \frac{(1-\theta_1)^2(\theta_4-4\theta_2^2)}{(1-\theta_2)^4} \right\} \quad (33a)$$

where

$$\theta_1 = \frac{1}{n} \sum_{i=1}^k n_{ii} , \quad (33b)$$

$$\theta_2 = \frac{1}{n^2} \sum_{i=1}^k n_{i+} n_{+i} , \quad (33c)$$

$$\theta_3 = \frac{1}{n^2} \sum_{i=1}^k n_{ii} (n_{i+} + n_{+i}) , \quad (33d)$$

$$\theta_4 = \frac{1}{n^3} \sum_{i=1}^k \sum_{j=1}^k n_{ij} (n_{j+} + n_{+i})^2 . \quad (33e)$$

Given the null hypothesis as

$$H_0: (K_1 - K_2) = 0, \quad (34a)$$

and the alternative hypothesis as

$$H_1: (K_1 - K_2) \neq 0, \quad (34b)$$

$H_0$  is rejected if  $z \geq z_\alpha$  where  $\alpha$  is the confidence level of the z test. It is most common to set  $\alpha$  as 0.05 or to set confidence level at 95%.

Since the error matrix does not provide an accuracy assessment measure for individual classes, conditional Kappa is computed. One can compute it for an individual species and apply the same comparison tests for the Kappa coefficient to this conditional Kappa. Conditional Kappa can be computed as

$$K_i = \frac{n \cdot n_{ii} - n_{i+} \cdot n_{+i}}{n \cdot n_{i+} - n_{i+} \cdot n_{+i}} \quad (35)$$

And the approximate variance for the  $i$ th category is computed as

$$\text{var}(K_i) = \frac{n(n_{i+} - n_{ii})}{[n_{i+} (n - n_{+i})]^3} [(n_{i+} - n_{ii})(n_{i+} n_{+i} - n n_{ii}) + n n_{ii} (n - n_{i+} - n_{+i} + n_{ii})] \quad (36)$$

Accordingly, Equation 34 and 33 are used to assess and compare the accuracy of individual tree species. Table 1 shows the classification of Kappa coefficient proposed by Landis & Koch (1977).

Table 1. Classification of Kappa coefficient. Source: Landis & Koch (1977)

Kappa coefficient	
0	Poor
0.00 - 0.20	slight
0.21 - 0.40	Fair
0.41 - 0.60	Moderate
0.61 - 0.80	Substantial
0.81 - 1.00	Almost perfect

This classification of Kappa can be used for interpretation of the result of classification for the further analysis.



## 4. MATERIAL AND STUDY AREA

### 4.1. Study area location:

The research has been done in the city of Delft in the province of South Holland, the Netherlands. The study area is located at 52° 01' 01.7" N 4° 21' 01.9" E, 52° 01' 02.3" N 4° 22' 09.6" E, 52° 00' 26.17" N 4° 22' 09.89" E, 52° 00' 25.6" N 4° 21' 02.6" E. Delft city has different species with large within species varieties (Chepkochei, 2014). In the study area, in total 4 main species have been detected.

### 4.2. Data

#### 4.2.1. Very high resolution aerial image

The image used for this research is a 25 cm by 25 cm high spatial resolution multi-spectral airborne imagery taken by in a sunny, clear conditions. The image comprises three spectral bands: blue (410-570 nm), green (480-630 nm), and red (570-700 nm).

Table 2. Characteristics of aerial image used for urban tree species classification.

Image	
Sensor	Ultracam XP
Acquisition date	09/06/2009
Local time	11:50 AM
Elevation angle (degree)	72.96
Solar zenith angle (degree)	17.04
Resolution (m)	0.25
Bands (nm)	blue (410-570), green (480-630), and red (570-700)

Figure 13 shows the study area covered by the aerial image.

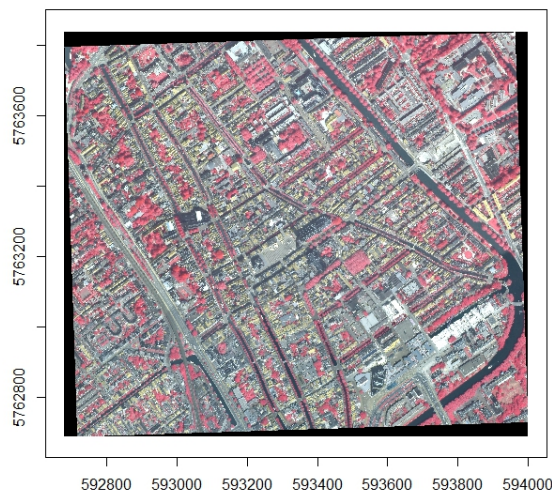


Figure 13. Study area within Delft city, RGB: green, red, and blue (2, 3, and 1)



#### 4.2.2. Reference data

Tree species information used as reference data has been collected from the Delft tree species guide by Dat et al. (2006) and the reference data set used in the research done by Chepkochei, (2014). The reference data has been divided into two sets; one to be used as training set and the other set for verification as shown in Table 3.

Table 3. Reference data used as training and verification sets.

Species	Number of tree crowns	
	Training set	Verification set
<i>Plantanus Spp.</i>	12	11
<i>Corylus Spp.</i>	6	6
<i>Alnus Spp.</i>	16	15
<i>Tillis Spp.</i>	48	48
Total	82	80

In this research, the total number of tree crowns is 162 (82 tree crowns for training set and 80 tree crowns for verification set). The largest data set is for *Tilia Spp.* and smallest data set is for *Corylus Spp.* All the tree crown polygons have been extracted manually. In addition, since interlocked tree crowns are not subject of this study, only single tree crowns have been delineated.

#### 4.3. Software

In this research, following software were used:

- ERDAS Imagine 2013, version 13.0.2 which was used for geo-referencing the study site;
- ArcGIS version 10 which was used for processing of referenced data;
- R version 3.0.2 which was used for statistical computing, graphics and data analysis.

In addition, following packages of R were used:

- geoR which is used for geostatistical analysis.
- rgdal which allow access to projection and transformation operations
- rgal which provides medium to high levels functions for 3D interactive graphics (Adler, et. al. , 2015).
- maptool which is used for manipulating and reading geographic data, in especially ESRI shape files.
- glcm which is used for computing GLCM texture measurements. In this research, this package has been used for computing pixel-wise GLCM texture measurements.
- lattice which is used for high level data visualization

## 5. RESULTS

### 5.1. Fitting surface models to spectral profile of crowns

This research has applied two methods, nonlinear regression and grid search, to fit surface models to the spectral profile of tree crowns. In this research, it has been observed that applying nonlinear regression for estimation of parameter  $n$  (crown curvature) of the Pollock model causes large errors due to the big deviations in parameter estimation of some tree crowns especially for *Corylus Spp.* In addition, iterative process of nonlinear regression has a high sensitivity to the starting values in a way that not well chosen starting values can stop the convergence at sub-optimal estimates.

Table 4 shows the accuracy of fit of these two methods in terms of root mean square error (RMSE). As one can see from the table, by applying grid search for fitting the surface model *Corylus Spp.* has the most improvement. According to Table 4, grid search performs more accurately for three species (*Plantanus Spp.*, *Corylus Spp.*, and *Tilia Spp.*) classes and performs as accurate as nonlinear regression for *Alnus Spp.* Therefore, grid search method is chosen for curve fitting.

Table 4. Root mean square error (RMSE) of fitting surface models to spectral profile of each species by applying two methods grid search and nonlinear regression.

	RMSE of grid search	RMSE of nonlinear regression
<i>Plantanus Spp.</i>	0.028	0.029
<i>Corylus Spp.</i>	0.041	0.046
<i>Alnus Spp.</i>	0.027	0.027
<i>Tilia Spp.</i>	0.032	0.034

To see how well each surface model fits the spectral profile of each species, root mean square error (RMSE) as a goodness of fit has been computed. In Table 5, results of fitting surface models to the spectral profile of each species by applying grid search has been shown. Accordingly, the best fit in terms of the lowest RMSE is provided by Pollock model for all four species. Therefore, Pollock model is chosen as the best model in terms of lowest RMSE for all species for further analysis.

Table 5. Root mean square error (RMSE) as a goodness of fit of surface models to spectral profile of each species

	RMSE of Pollock model	RMSE of Gaussian model	RMSE of Paraboloid model
<i>Plantanus Spp.</i>	0.028	0.034	0.032
<i>Corylus Spp.</i>	0.041	0.045	0.048
<i>Alnus Spp.</i>	0.027	0.033	0.043
<i>Tilia Spp.</i>	0.032	0.043	0.051

Table 6 shows estimated Pollock parameters and confidence interval on mean of each parameter (refers to section 3.3.7). As one can see from Table 6 and Table 2, variability decreases as sample size increases. Therefore, *Tilia Spp.* with the largest sample size has the lowest standard error for the estimates of  $a$ ,  $b$  and  $n$  while *Corylus Spp.* with the smallest sample size has the largest variability in estimate of mean of each parameter. However, for *Corylus Spp.* this large variability does not seem to be problematic for classification

since its ranges especially for  $n$  and  $a$  parameter are well separated from the range of other species. In addition, *Corylus Spp.* has the largest values for parameter  $n$  and spectral profile for this species is closer to a cylinder shape whereas *Tilia Spp.* has the lowest  $n$  parameter and the shape of its spectral profile is closer to a conical shape.

Table 6. Standards error of mean and confidence interval for mean of Pollock parameters for each species.

	$SE_n$	95% CI on $\mu_n$	$SE_a$	95% CI on $\mu_a$	$SE_b$ (m)	95% CI on $\mu_b$ (m)
<i>Plantanus Spp.</i>	0.17	$1.72 < \mu_n < 2.07$	0.01	$0.21 < \mu_a < 0.23$	0.72	$7.86 < \mu_b < 9.30$
<i>Corylus Spp.</i>	0.33	$2.09 < \mu_n < 2.75$	0.02	$0.32 < \mu_a < 0.36$	1.74	$6.99 < \mu_b < 10.48$
<i>Alnus Spp.</i>	0.13	$1.60 < \mu_n < 1.86$	0.01	$0.22 < \mu_a < 0.24$	0.22	$4.60 < \mu_b < 5.03$
<i>Tilia Spp.</i>	0.06	$1.53 < \mu_n < 1.65$	0.01	$0.25 < \mu_a < 0.26$	0.21	$4.41 < \mu_b < 4.83$

Figure 14 shows the uncertainty of fit for one crown (refers to section 3.3.8). As one can see from Figure 14, fitting the Pollock model has the highest sensitivity to parameter  $a$ , by considering a tolerance of 0.01. This means that any small error in estimating parameter  $a$  can cause a large error in fitting the Pollock model to the spectral profile. One possible reason could be the high precision which is needed for estimating parameter  $a$  since it ranges from 0.0 to 0.4. In addition, as we get far from the optimum value for  $a$  and  $b$  the rate of change in RMSE is the same for both parameters, and both for values larger and smaller than the optimum value. However, parameter  $n$  has different behaviour in such a way that the rate of change in RMSE for values smaller than optimum  $n$  is higher than it is for values larger than optimum  $n$ . This means that the possibility of error caused by overestimating  $n$  is larger than underestimating it in a given tolerance.

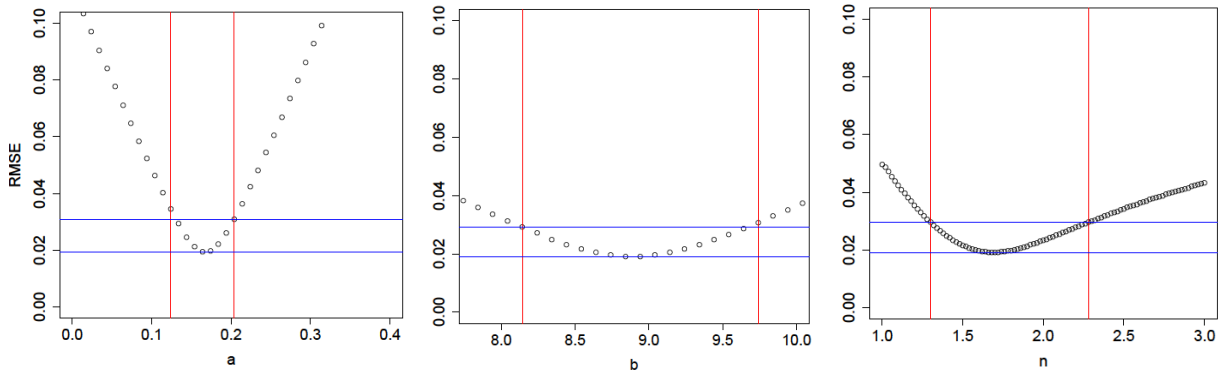


Figure 14. From left to right changing accuracy (RMSE) by changing parameters  $a$ ,  $b$ , and  $n$  for fitting Pollock model to spectral profile of a crown. This figure shows how accuracy (RMSE) of fitting Pollock model changes with parameter  $a$ ,  $b$  and  $n$ . Pollock has the highest sensitivity to parameter  $a$  and any small changes in  $a$  can make large changes in RMSE.

Figure 15 shows how information extracted from the fitting the Pollock model matches and describes the real shape of each tree species. As one can see from the figure, *Corylus Spp.* has a dense crown which justifies its large value for parameter  $a$  compared to other species. In addition, it is also dense at its crown boundary that justifies the cylindrical shape of its spectral profile and large value for parameter  $n$ . On the other hand, *Tilia Spp.* is denser in the centre of its crown than at its boundary which explains the conical shape of its spectral profile.

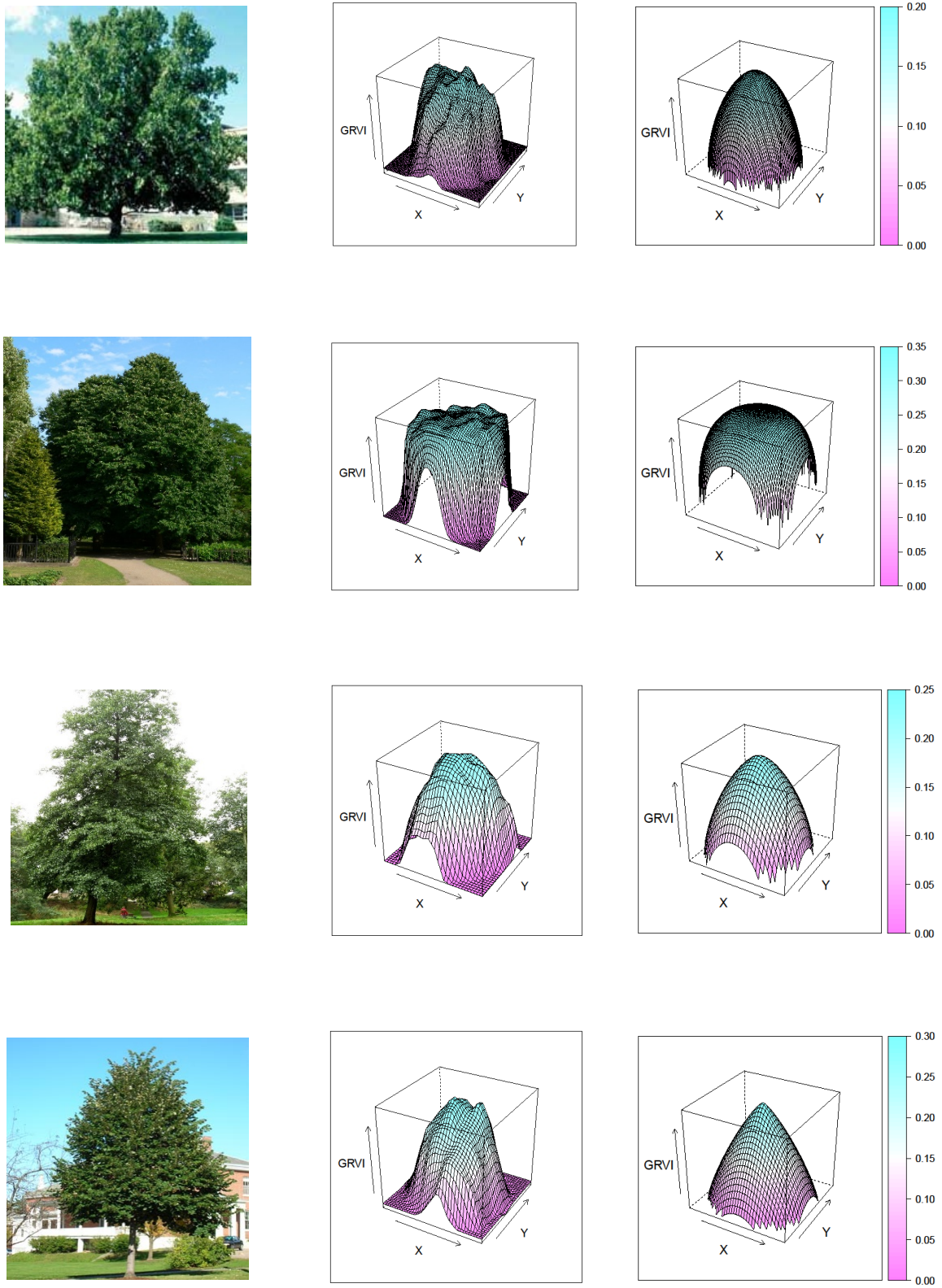


Figure 15. Shape information for each tree species. From left to the right: the real shape of a tree, spectral profile and fitted Pollock model to the spectral profile, respectively. From top to bottom: *Plantanus Spp.*, *Corylus Spp.*, *Alnus Spp.*, and *Tilia Spp.*, respectively. This figure shows how real shape of each tree species matches its spectral profile and the fitted Pollock model.

Figure 16 shows the boxplots of estimated parameters of the Pollock model ( $a$ ,  $b$ , and  $n$ ). In the figure, the thick black line shows the median and the cross sign represents the mean of each parameter distribution. According to the figure, mean and median have approximately similar values. The boxplots for parameters suggest that data are symmetrically distributed. The median lies approximately in the middle of the box and the whiskers are approximately the same length. Therefore, according to the boxplots and other normality tests (histogram and qq-plot), estimated parameters for each species are approximately normally distributed.

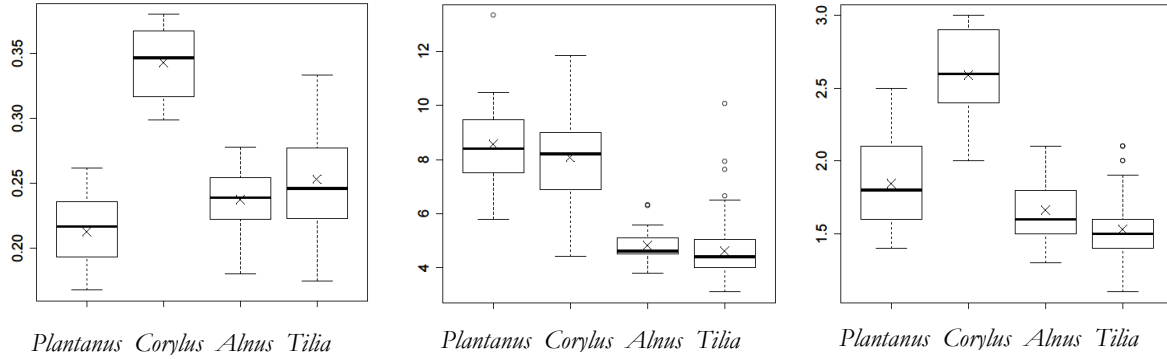


Figure 16. Boxplots of Pollock parameters for each species. From left to right boxplots for estimated parameter  $a$ , estimated parameter  $b$ , estimated parameter  $n$ . The thick black line shows the median and the cross sign represents the mean of each parameter distribution.

## 5.2. Maximum Likelihood Classification (MLC) based on Pollock parameters

Since the estimated parameters for each species approximate normal distributions, an appropriate classifier that can be used to discriminate different species based on the Pollock parameters is Maximum Likelihood classification.

Parameters  $a$  and  $n$ , refer to Equation 12, which correspond to the height and shape of spectral profile, respectively, can be used as descriptors of tree species. However, parameter  $b$  which represents the size of crowns is subject to broad variation. According to Table 6, for all species parameter  $b$  has the highest standard error compared to parameters  $a$  and  $n$ . The reasons for this large variation can be differences in age of trees and pruning of tree crowns. To see if parameter  $b$  can improve the classification, one classification just considers parameters  $a$  and  $n$  while the other classification also adds parameter  $b$ .

Table 7. Comparison of Kappa coefficient for two classifications, one based on parameters  $a$  and  $n$  as the descriptors and the other one by addition of parameter  $b$ .

Classification #1	Classification #2	$K_1$	Var ( $K_1$ )	$K_2$	Var ( $K_2$ )	$ z $	p-value	Significant?
Pollock parameters $a$ and $n$	Pollock parameters $a$ , $b$ , and $n$	0.27	0.006	0.53	0.007	2.28	0.01	Yes

According to Table 7, by addition of parameter  $b$  for classification, Kappa coefficient has significantly increased and classification has improved. To see for which species Kappa coefficient shows large improvement by adding parameter  $b$ , conditional Kappa for each species has been computed as well. The results are presented in Table 8.

Table 8. Conditional Kappa coefficients for two classifications, one based on parameters **a** and **n** as descriptors and the other one by addition of parameter **b**.

	Descriptor (feature)	<i>Plantanus Spp.</i>	<i>Corylus Spp.</i>	<i>Alnus Spp.</i>	<i>Tilia Spp.</i>
Classification #1	Pollock parameters <b>a</b> and <b>n</b>	0.14	1.00	0.16	0.46
Classification #2	Pollock parameters <b>a</b> , <b>b</b> , and <b>n</b>	0.75	1.00	0.24	0.57

Table 8 shows that addition of parameter **b** has the largest effect on classification of *Plantanus Spp.* and has no effect on *Corylus Spp.* Since *Corylus Spp.* has the highest value for **n** and is completely distinct from the other species in terms of **n**, addition of another descriptor like **b** does not influence its classification. However, for other species addition of **b** has improved classification.

Table 9 shows the class separability based on the Pollock parameters (**a**, **b** and **n**). According to the table, the highest class separability is between *corylus Spp.* and *Alnus Spp.* (1.99) and lowest class separability is between *Alnus Spp.* and *Tilia Spp.* (0.66).

Table 9. Class separability (transformed divergence) between tree species based on Pollock parameters **a**, **b** and **n** as descriptors

	<i>Plantanus Spp.</i>	<i>Corylus Spp.</i>	<i>Alnus Spp.</i>	<i>Tilia Spp.</i>
<i>Plantanus Spp.</i>	0.00	1.92	1.98	1.92
<i>Corylus Spp.</i>	1.92	0.00	1.99	1.97
<i>Alnus Spp.</i>	1.98	1.99	0.00	0.66
<i>Tilia Spp.</i>	1.92	1.97	0.66	0.00

Table 10 and 11 show the results of contingency analysis of training set and verification set based on Pollock parameters. As expected, classification of training set has high accuracy.

Table 10. Contingency analysis of training set based on Pollock parameters (**a**, **b**, and **n**)

	<i>Plantanus Spp.</i>	<i>Corylus Spp.</i>	<i>Alnus Spp.</i>	<i>Tilia Spp.</i>	User accuracy (%)	Overall accuracy (%)
<i>Plantanus Spp.</i>	12	0	0	0	100	71.95
<i>Corylus Spp.</i>	0	6	0	1	86	
<i>Alnus Spp.</i>	0	0	12	18	40	
<i>Tilia Spp.</i>	0	0	4	29	88	
Producer accuracy (%)	100	100	75	60		
Kappa	0.58					

Table 11. Contingency analysis of verification set based on Pollock parameters ( $a$ ,  $b$ , and  $n$ )

	<i>Plantanus Spp.</i>	<i>Corylus Spp.</i>	<i>Alnus Spp.</i>	<i>Tilia Spp.</i>	User accuracy (%)	Overall accuracy (%)
<i>Plantanus Spp.</i>	11	0	2	1	79	71.25
<i>Corylus Spp.</i>	0	4	0	0	100	
<i>Alnus Spp.</i>	0	0	8	13	38	
<i>Tilia Spp.</i>	0	2	5	34	83	
Producer accuracy (%)	100	67	53	71		
Conditional Kappa	0.75	1.00	0.24	0.57		
Kappa	0.53					

### 5.3. Maximum Likelihood Classification (MLC) based on Pollock parameters and semivariogram model

Figure 17 shows the extraction of semi-variogram from fine structure of a tree crown and fitting a model to it. In the figure, normality of distribution of fine structure has been tested. Since the histogram and the qq-plot plot suggest that data are normally distributed, one can assume that the trend in the fine structure is just a function of the coordinates and not an external variable. As one can see from the figure, sample variogram values tend to become erratic at long lags since at longer lags data tends to be less correlated.

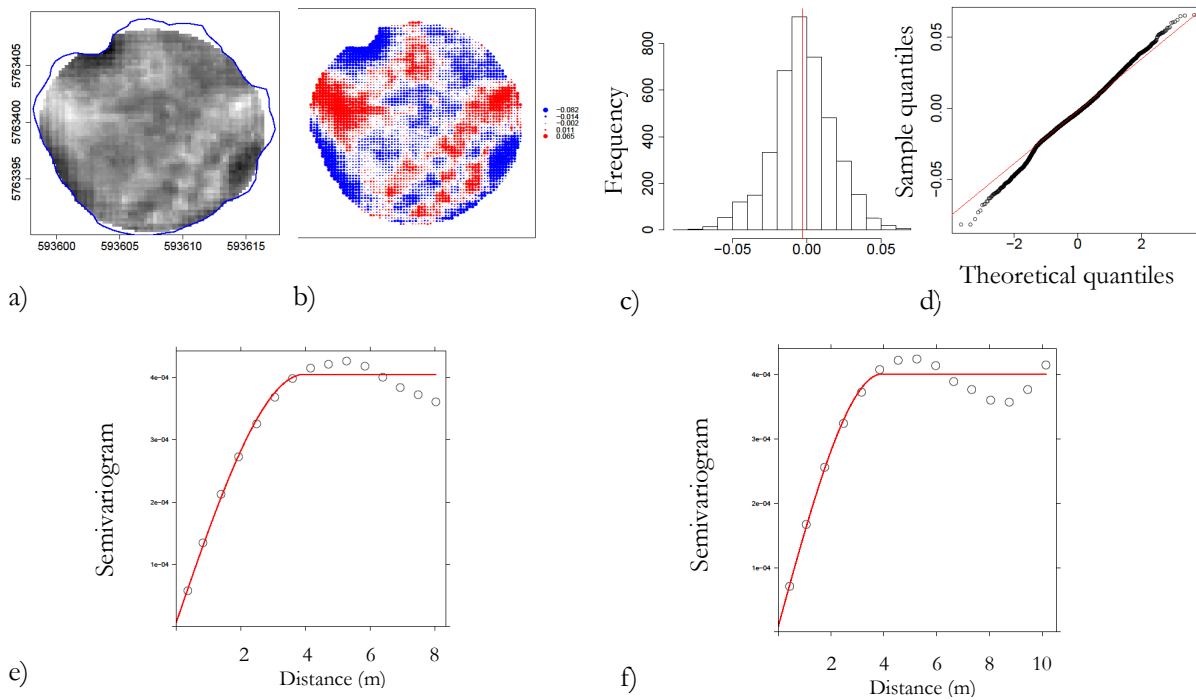


Figure 17. Extracting semi-variogram from fine structure of a crown and fitting a variogram model. a) fine structure of a crown, b) fine structure as geostatistical data c) histogram of fine structure of a crown; red line shows the mean of distribution, d) qqplot of fine structure; red line shows the normal distribution, e) variogram up to the lag of 8 m; red curve shows the fitted model, f) variogram up to the lag of 10 m; red curve shows the fitted model.

Figure 18 shows the distribution of parameters extracted from fitted variogram model for each species. In the figure, thick black line and cross sign show median and mean of each parameter, respectively. The boxplots suggest that sill and effective range are approximately normally distributed for most of tree species. The slope is computed by division of partial sill by the effective range. As Figure 18 shows, slope does not add extra information. Therefore, for classification just the two parameter range and sill are selected as the descriptors.

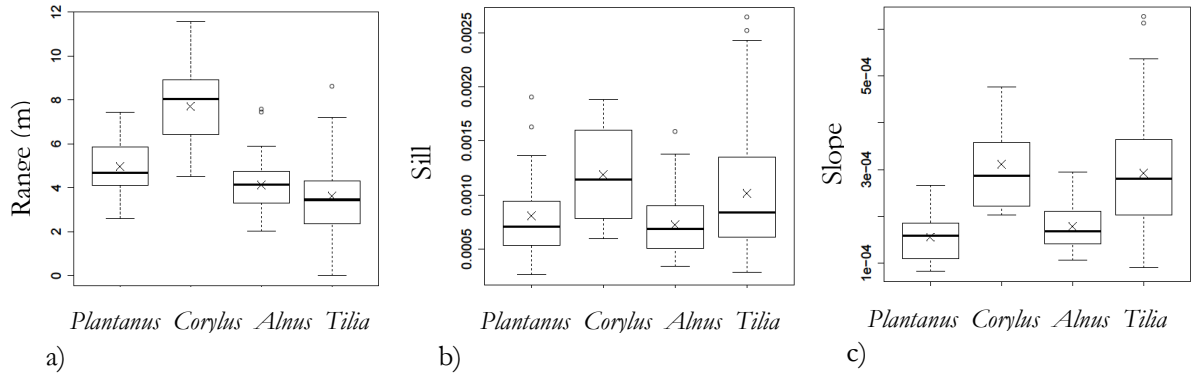


Figure 18. Distribution of parameters extracted from fitted variogram model for each species. From left to right a) effective range in meter, b) sill , c) slope which is computed by division of the partial sill by the range.

The third classification is based on the extracted parameters from a fitted semi-variogram model (sill and range) and the Pollock parameters. The variogram range measures the texture coarseness and is related to the size of the textural features and sill is proportional to the global variance of the textural feature. Table 12 shows the contingency analysis of the validation set.

Table 12. Contingency analysis of the verification set based on the Pollock parameters and semi variogram model

	<i>Plantanus Spp.</i>	<i>Corylus Spp.</i>	<i>Alnus Spp.</i>	<i>Tilia Spp.</i>	User accuracy	Overall accuracy
<i>Plantanus Spp.</i>	10	0	2	1	77	73.75
<i>Corylus Spp.</i>	0	4	0	0	100	
<i>Alnus Spp.</i>	1	0	9	11	43	
<i>Tilia Spp.</i>	0	2	4	36	86	
Producer accuracy	91	67	60	75		
Conditional Kappa	0.73	1.00	0.30	0.64		
Kappa	0.56					

Table 13 represents the results of the Kappa analysis that compares the contingency matrices of two classifications, one only based on the three Pollock parameters ( $a$ ,  $b$  and  $n$ ) and the other one by addition of semivariogram parameters ( sill and range).

Table 13. Comparison of Kappa coefficient for two classification, one based on Pollock parameters ( $a$ ,  $b$  and  $n$ ) and the other one by addition of semivariogram parameters ( sill and range).

Classification #2	Classification #3	$K_2$	Var ( $K_2$ )	$K_3$	Var ( $K_3$ )	$ z $	Significant?
Pollock	Pollock + semivariogram	0.53	0.0070	0.56	0.0068	0.25	NO



The significance level for rejecting the null hypothesis is set as 0.05. Table 13 shows that although addition of two parameters extracted from the semivariogram model has improved classification in terms of Kappa coefficient, this improvement is not significant.

#### 5.4. Maximum Likelihood Classification (MLC) based on Pollock parameters and GLCM texture measurements

Figure 19 represents object-wise GLCM texture measurements (refer to 3.7) in different lags for each tree species. In this figure, for each species the average of texture measurements for all crowns has been computed. As Figure 19 shows, object-wise GLCM texture measurements are functions of lag.

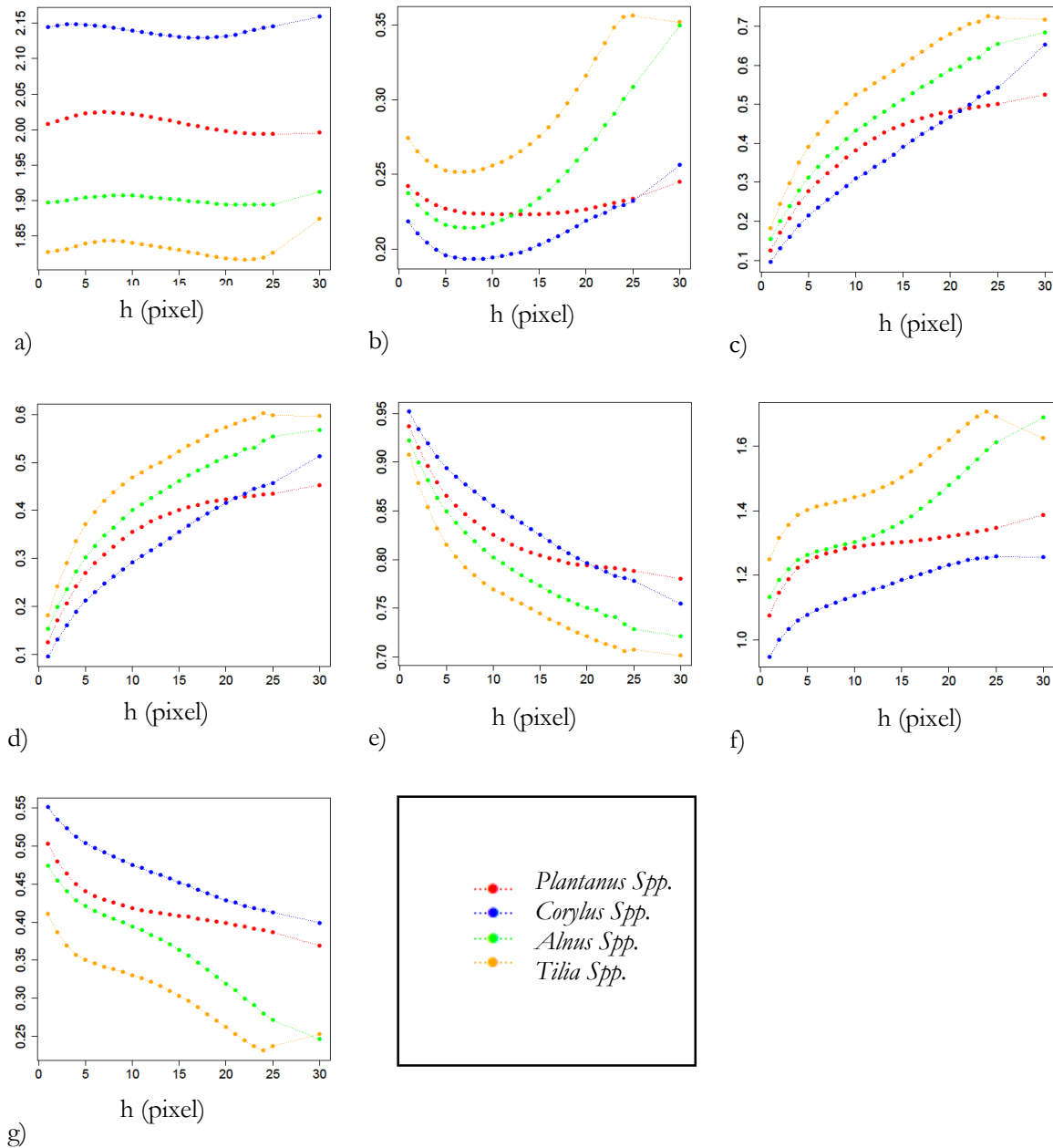


Figure 19. GLCM measurements as a function of lag by applying a global (object-wise) window for computing GLCM matrix. a) mean, b) variance, c) contrast, d) dissimilarity, e) homogeneity, f) entropy, g) angular second moment. The figure shows the dependence of the GLCM texture measurements on the lag. In this figure dashed lines are for visual interpretation purpose.

To choose the most suitable lag for classification one needs to compute class separability for each lag for each pair of species. Figure 20 shows the results of computing transformed divergence (TD) up to the lag of 30 pixels.

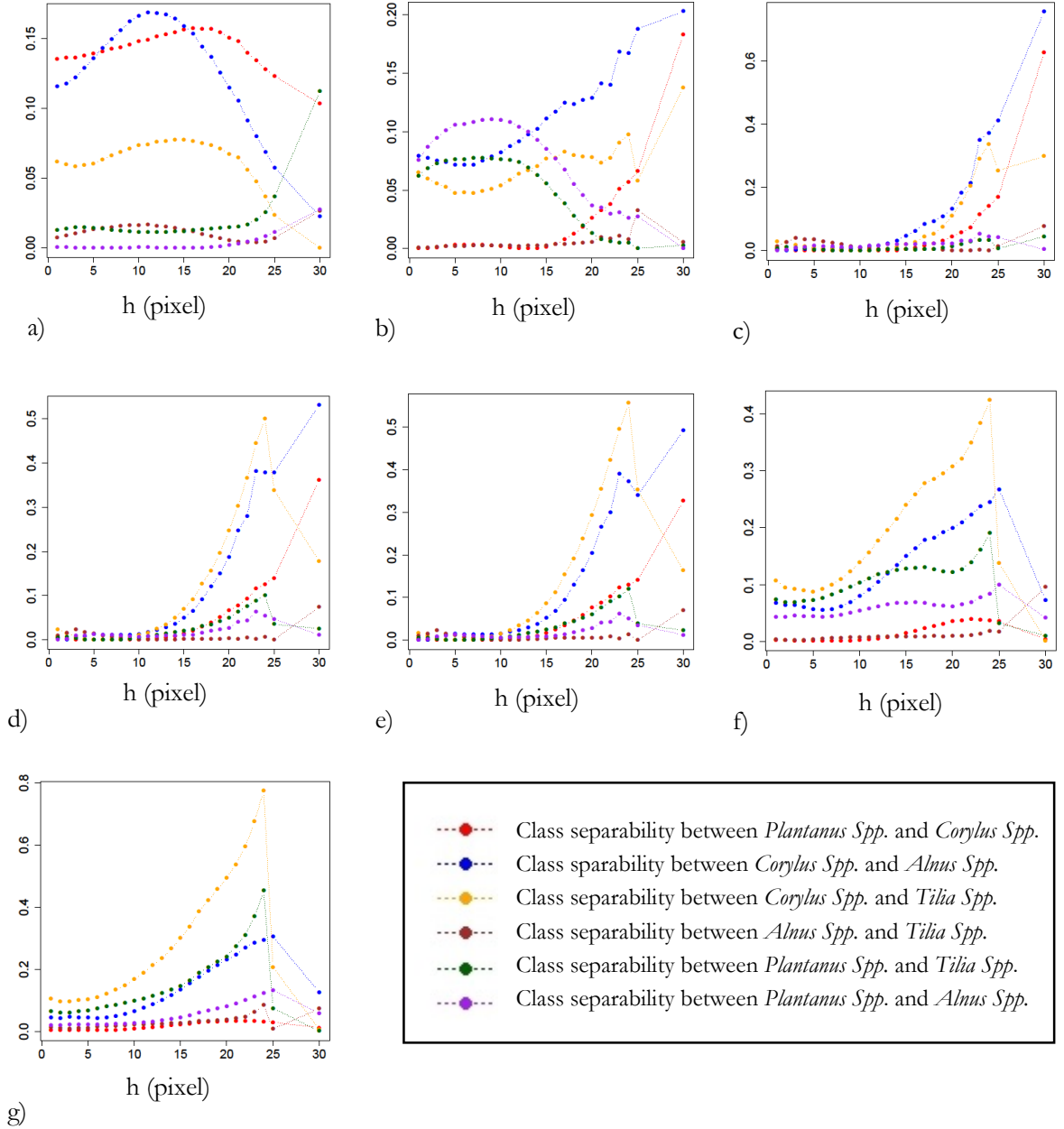


Figure 20. Transformed divergence (TD) of GLCM texture measurements for each pair of species. a) mean, b) variance, c) contrast, d) dissimilarity, e) homogeneity, f) entropy, g) angular second moment. In this figure dashed lines are for visual interpretation purpose.

Since *Tilia Spp.* has the smallest crown diameter and the average parameter  $b$  for *Tilia Spp.* representing the radius of tree crown estimated by fitting Pollock model is 3.1 m, by computing GLCM matrix for the lags more than 24 pixels one will lose a large number of data for this species. Therefore, for choosing the most suitable lag in terms of highest separability one should choose the lags smaller the crown diameter, in this case smaller than 24 pixel.

As Figure 20 shows, for some texture measures like angular second moment, entropy, homogeneity, and dissimilarity finding the lag that gives best separability is possible by visual interpretation (in this case lag 24) since for these texture measures different species have approximately the same behaviour. However, for some texture measurements like mean and variance it is not possible by visual interpretation as different species have completely different behaviour. In this case, one can choose the lag which provides the best separability for the specific species with the lowest class separability. In this research transformed divergence of mean and variance for *Tilia Spp.* and *Alnus Spp.* having the lowest class separability, which does not change much with lag. Therefore, by applying a classification based on each texture measurement in different lags, the lag providing the largest Kappa (lag 15 for mean and 13 for variance) have been chosen.

Table 14 shows the correlation between the texture measurements. Considering the high correlation between the texture measurements, those texture measures which provide the highest separability compared to their correlated measures are selected. Therefore classification is limited to only mean at lag 15 and angular second moment at lag 24 as the descriptors.

Table 14. Correlation between texture measurements of for *Plantanus Spp.*

	Mean	Variance	Contrast	Dissimilarity	Homogeneity	Entropy	Angular second moment
Mean	1.00	0.96	-0.67	-0.65	0.65	0.48	0.47
Variance	0.96	1.00	-0.67	-0.65	0.65	-0.48	0.47
Contrast	-0.67	-0.67	1.00	0.99	-0.99	0.98	-0.96
Dissimilarity	-0.65	-0.65	0.99	1.00	-0.99	0.99	-0.97
Homogeneity	0.65	0.65	-0.99	-0.99	1.00	-0.97	0.97
Entropy	0.48	-0.48	0.98	0.99	-0.97	1.00	-0.99
Angular second moment	0.47	0.47	-0.96	-0.97	0.97	-0.99	1.00

Table 15 shows the results of maximum likelihood classification based on the Pollock parameters and the GLCM texture measurements computed from a global (object-wise) window (refers to 3.7).

Table 15. Contingency analysis of classification base on the Pollock parameters and GLCM texture measurements computed from an object-wise window.

	<i>Plantanus Spp.</i>	<i>Corylus Spp.</i>	<i>Alnus Spp.</i>	<i>Tilia Spp.</i>	User accuracy	Overall accuracy
<i>Plantanus Spp.</i>	11	0	1	0	92	73.75
<i>Corylus Spp.</i>	0	1	0	0	100	
<i>Alnus Spp.</i>	0	0	10	11	48	
<i>Tilia Spp.</i>	0	5	4	37	80	
Producer accuracy	100	17	67	77		
Conditional Kappa	0.90	1.00	0.36	0.51		
Kappa	0.55					

Another classification has been done based on Pollock parameters and GLCM texture measurements computed from a pixel wise window. Since by applying a pixel wise GLCM texture measurement for each pixel there is a GLCM matrix and a corresponding texture measurement, for each crown the average of texture measures have been computed (refer to section 3.8). Then the most separable lag and window size has been selected. For this research, pixel wise GLCM mean at lag 8 and homogeneity at lag 7 has been chosen for classification. Table 16 shows the results of this classification.

Table 16. Contingency analysis of classification base on the Pollock parameters and GLCM texture measurements computed from pixel-wise window.

	<i>Plantanus Spp.</i>	<i>Corylus Spp.</i>	<i>Alnus Spp.</i>	<i>Tilia Spp.</i>	User accuracy	Overall accuracy
<i>Plantanus Spp.</i>	11	0	3	0	79	71.25
<i>Corylus Spp.</i>	0	5	0	1	83	
<i>Alnus Spp.</i>	0	0	8	14	36	
<i>Tilia Spp.</i>	0	1	4	33	87	
Producer accuracy	100	83	53	69		
Conditional Kappa	0.75	0.82	0.22	0.67		
Kappa	0.55					

As one can see from Table 16 and 15 the Kappa coefficient is the same for both pixel wise and object wise GLCM texture measurements classifications.

### 5.5. Classification based on GLCM texture measurements profiles

Another suggested approach for classification was based on the profile of a texture measurement (refer to section 3.8). As one can see from Figure 21, since between classes variation is not more than within class variation, this approach fails to be used for classification.

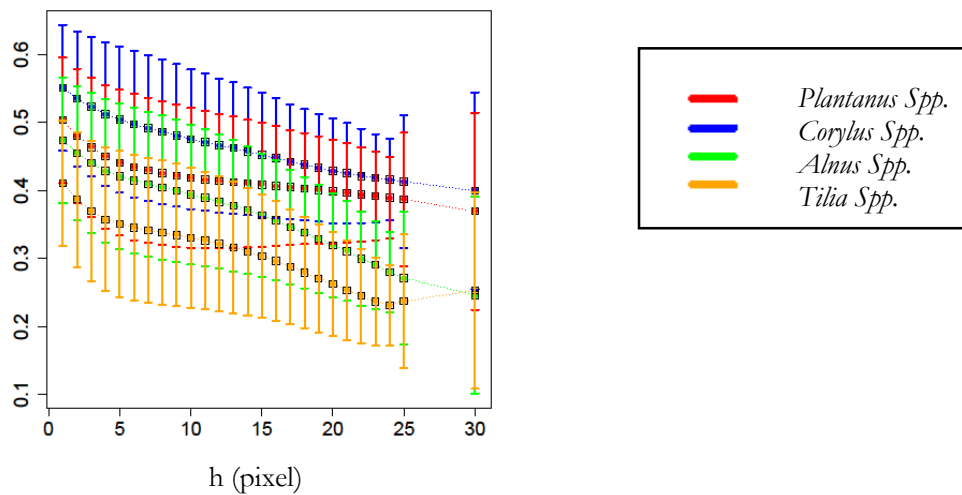


Figure 21. Mean and standard deviation of object-wise GLCM angular second moment (texture measurement) for each species. In the figure, the squares show the mean and error bars show the within class variation.

### 5.6. Summary of Classification

So far, all the classifications have been applied on the fine structure of the spectral profile. To see whether the fine structure adds additional information for classification compared to the spectral profile, two object wise GLCM texture measurements classifications, one base on the fine structure and the other one based on the spectral profile, have been applied. Table 17 shows the comparison of Kappa coefficient for these two classifications.

Table 17. Comparison of Kappa coefficient for two classification, one based on object wise GLCM texture measurements of fine structure and the other one based on the object wise GLCM texture measurements of the spectral profile.

Classification #6	Classification #7	K <sub>6</sub>	Var (K <sub>6</sub> )	K <sub>7</sub>	Var (K <sub>7</sub> )	z	Significant?
GLCM texture measures of fine structure	GLCM texture measures of spectral profile	0.19	0.0055	0.14	0.0052	0.48	NO

Table 17 shows that using fine structure instead of spectral profile has been improved classification accuracy. However, this improvement is not significant.

Table 18 shows the Kappa coefficient and conditional Kappa for all classifications which have been applied.

Table 18. Kappa coefficient for each classification and conditional Kappa for each species.

#	Maximum Likelihood Classification approach based on	Kappa	Conditional Kappa			
			<i>Plantanus Spp.</i>	<i>Corylus Spp.</i>	<i>Alnus Spp.</i>	<i>Tilia Spp.</i>
1	Pollock parameters <i>a</i> and <i>n</i>	0.27	0.14	1.00	0.16	0.46
2	Pollock parameters <i>a, b</i> and <i>n</i>	0.53	0.75	1.00	0.24	0.57
3	Pollock parameters ( <i>a, b, n</i> ) and semi vairogram parameters (sill, range)	0.56	0.73	1.00	0.30	0.64
4	Pollock parameters ( <i>a, b, n</i> ) and object-wise GLCM texture measures	0.55	0.90	1.00	0.36	0.51
5	Pollock parameters ( <i>a, b, n</i> ) and pixel-wise GLCM texture measures	0.55	0.75	0.82	0.22	0.67
6	object-wise GLCM texture measures of fine structure	0.19	0.21	0.28	0.09	0.41
7	object-wise GLCM texture measures of spectral profile	0.14	0.17	0.19	0.01	0.36

According to the Table 18, high accuracy of *Corylus Spp.* is due to Pollock parameters in a way that in all classification that Pollock parameters have been used *Corylus Spp.* has the largest conditional Kappa. However, in the classifications that only textural information have been used *Corylus Spp.* is easily confused with other species. In contrast, *Tilia Spp.* has the highest classification accuracy in all classifications that only textural information have been used.

As one can see from the table, classification based on the Pollock parameters (*a, b, n*) and semi vairogram parameters (sill, range) has the largest Kappa coefficient (0.56) compared to other classifications. By addition of the semi vairogram parameters to the Pollock paremeters, *Tilia Spp.* has the most improvement.

## 6. DISCUSSION

### 6.1. Fitting surface models to spectral profile of crowns

The study shows that spectral profile is a property that can be used for classification of four main species (*Plantanus Spp.*, *Corylus Spp.*, *Alnus Spp.*, and *Tilia Spp.*) in an urban area in Delft city, The Netherlands. According to the classification of Kappa coefficient (refer to Table 1), *Corylus Spp.* has been classified almost perfectly; *Plantanus Spp.* has been classified substantially; *Tilia Spp.* has been classified moderately and *Alnus Spp.* has been classified fairly.

Success in classification of *Corylus Spp.* is of crucial importance since in the research done by Chepkochei (2014) *Corylus Spp.* was easily confused by *Tilia Spp.* whereas by considering spectral profile parameters instead of multispectral signature *Corylus Spp.* is completely separable from other species, in particular *Tilia Spp.* Furthermore, the classification success of *Plantanus Spp.* is important since this species is commonly used as ornamental trees in urban areas (Turner et. al., 2012).

In this research, tree crown polygons have been delineated manually. The manual procedure of tree crown delineation would not be applicable for the other study areas with the large number of trees. Automatic delineation of tree crowns is an alternative method which is faster and cost efficient. However, it is less accurate than manual procedure and may cause additional errors which will affect the analysis. Several object based methods have been developed to detect individual crown boundary automatically (e.g. Gougeon & Leckie, 2003, Gougeon, 1995a). Ardila et al. (2012a) developed object based methods for identification of individual trees in urban areas that can be used as an alternative for automatic delineation of tree crowns.

In this research, an assumption has been made that geometric model of the tree crown surface can be applied for the radiometric model of the tree crown due to constant density of leaves inside the tree crown. This assumption has been used for both sun illumination correction and for modelling the coarse structure of the spectral profile. The comparison of the real shapes of the tree crowns, corresponding spectral profiles and fitted models for each tree species has proven the validity of this assumption for the tree species studied in this research.

Since illumination conditions are more evident in airborne rather than spaceborne data (Ardila, 2012), C-correction has been applied for correcting the effects of uneven sun illumination in this research (refer to 3.3.2). This method has been applied on the Green Red Vegetation Index (GRVI) rather than the original image bands. The vegetation indices are the relative measures and partially correct the uneven sun illumination effects. Accordingly, in the research done by Ardila, (2012) the vegetation index was considered as the uneven sun illumination correction. However, vegetation indices can only compensate the effect of sun illumination geometry which is the same for all the bands of the image and does not correct the effect of topography. In this research, since the solar zenith angle is  $17.04^\circ$ , the effect of sun illumination geometry is not such strong to affect the spectral profiles of the tree crowns. Therefore C-correction on GRVI has worked well enough. However, applying both vegetation index and correction for the effect of sun illumination geometry can cause problems for the images acquired with different solar zenith angle which have much stronger sun illumination effect.

Since the spectral profile of the tree crowns generally form a bell-curved surface, Pollock, Gaussian, and Paraboloid models have been used for modelling of coarse structure. Fitting parameter  $n$  (crown curvature)

of the Pollock model by nonlinear regression causes large errors due to the big deviations in parameter estimation of some tree crowns since the iterative procedure might be trapped in the local minimum. Consequently, one needs to use different sets of starting values to protect against local minima. In addition, iterative process has a high sensitivity to the starting values in a way that not well chosen starting values can stop the convergence. As an alternative, grid search has been proposed, based on the pre-knowledge about the possible ranges for each parameter. Although grid search performs more accurately for three species (*Plantanus Spp.*, *Corylus Spp.*, and *Tilia Spp.*) classes and performs as accurate as nonlinear regression for *Alnus Spp.*, the accuracy of grid search depends on precision with which these variables are defined. Consequently, for obtaining higher accuracy, one needs to increase the precision of the possible values of the grid which will increase computation time due to the large number of computations. For this research, the precision of one decimal number for parameter  $n$  and two decimal numbers for parameter  $a$  and  $b$  have been considered sufficient.

RMSE as a goodness of fit has shown that Pollock model can best approximate the spectral profile characteristic of tree crowns for all four species, as compared to the Gaussian and the Paraboloid models. It is an explanation of the better fit of the Pollock model because of its unique characteristics in defining the shape curvature by parameter  $n$ , denoted also as shape parameter. For *Corylus Spp.*,  $n$  tends to values of more than 2 and the fitted Pollock model tends to a cylindrical shape whereas for *Tilia* and *Alnus Spp.* parameter  $n$  tends to value 1 and the fitted Pollock model approximates a conical shape.

It has been observed that the accuracy (RMSE) of fitting the spectral profile by the Pollock model is more sensitive to parameter  $a$  compared to the other parameters. This means that any small error in estimating parameter  $a$  can cause a large error in the fitting of the Pollock model. As a result, for estimating of parameter  $a$  high precision is needed. However, determining the most critical parameter for fitting the Pollock model depends on the chosen vegetation index or band for extracting of the spectral profile and its corresponding range and precision. Therefore, one should not expect to obtain the same result when the spectral profile is obtained from another vegetation index with a different range.

The study shows that different tree species with different geometrical shape of the tree crowns show different spectral profiles which can be described by the Pollock parameters  $a$ ,  $b$ , and  $n$ . In this regard,  $a$  and  $b$  refers to the height of spectral profile and the radius of crown respectively and  $n$  represents the shape curvature of the spectral profile. The study shows that the geometrical shape a tree crowns matches the shape of its corresponding spectral profile. For example, in reality, *Corylus Spp.* has a dense crown which justifies its large value for mean of parameter  $a$  ranging from 0.32 to 0.36 with 95% confidence interval. It is also dense in crown boundary which justifies its large value for mean of parameter  $n$  ranging from 2.09 to 2.75 and the cylindrical shape of its spectral profile. On the other hand, *Tilia* and *Alnus Spp.* are denser in the centre of the crown than at its boundary which describes their range for mean of parameter  $n$  ranging from 1.60 to 1.86 and from 1.53 to 1.65 respectively and their conical shape of their spectral profile. Furthermore, *Plantanus Spp.* approximates an ellipsoidal shape which can be described by its values for mean of parameter  $n$  ranging from 1.72 to 2.07.

## 6.2. Maximum Likelihood Classification (MLC) based on Pollock parameters

The lowest class separability (transformed divergence) is 0.66 between *Tilia Spp.* and *Alnus Spp.* and the highest is 1.99 between *Corylus Spp.* and *Alnus Spp.* In particular *Corylus Spp.* shows high class separability with a measure of 1.9, 1.99, and 1.97 from *Plantanus Spp.*, *Alnus Spp.*, and *Tilia Spp.* respectively. The reason is that *Corylus Spp.* has the highest values for parameter  $n$  and  $a$  and is completely separable from the other species. On the other hand, *Tilia* and *Alnus Spp.* have close values for parameters  $n$ ,  $a$  and  $b$ , so they have the lowest class separability.

Addition of parameter  $b$  as a feature for classification has the most effect for *Plantanus Spp.* causing an increase in Kappa from 0.14 to 0.75. By considering parameters  $a$  and  $n$  for classification, *Plantanus Spp.* has low separability from *Tilia Spp.* and *Alnus Spp.* However, the radius of *Plantanus Spp.* ranging from 7.86 m to 9.30 m is completely distinctive from *Tilia Spp.* with an average of 4.8 m and *Alnus Spp.* with an average of 4.62 m. Although for this research and this specific tree species the addition of parameter  $b$  has improved the results of classification significantly, size of crowns is not always an appropriate feature for classification due to different age of trees and pruning of tree crowns.

In addition, from the Pollock parameters  $a$ ,  $b$ , and  $n$  more information than just the tree species classes can be extracted like age, health and sub-species variation. Once the tree species are classified, one can interpret the age of trees based on the parameter  $b$  and  $a$ . Also, one can extract information about the health of tree crowns based on the parameter  $n$  and  $a$  since tree diseases can affect the shape of a tree crown or density of leaves in a tree crown.

### 6.3. Maximum Likelihood Classification (MLC) based on Pollock parameters and texture measurements

The study shows that texture is a property that can be used as additional information for improving the classification of four main species (*Plantanus Spp.*, *Corylus Spp.*, *Alnus Spp.*, and *Tilia Spp.*) in an urban area in Delft city, The Netherlands. Accordingly, by applying classification based on object wise texture measurements and Pollock parameters, *Corylus Spp.* and *Plantanus Spp.* has been classified almost perfectly with conditional Kappa 1 and 0.9 respectively, *Tilia Spp.* has been classified moderately, and *Alnus Spp.* have been classified fairly.

For classification based on object wise GLCM texture measurements, it has been observed that there is not necessarily an optimum lag providing the highest class separability for all tree species. Although for GLCM angular second moment, dissimilarity, homogeneity, and entropy by computing class separability for each lag one can detect the most appropriate lag, for GLCM mean and variance different tree species might have different behaviour and there might not be an optimal lag. In this case, one should focus on those species whose classification accuracy needs to be improved.

In this research, the GLCM texture measurements have been computed at the same lag, optimum lag, for all tree species. However, different tree species may have different optimum lags. This might be the reason why by addition of pixel wise GLCM mean at lag of 8 pixels (2 m) and homogeneity at lag of 7 (1.75 m), *Tilia Spp.* has improved classification whereas by addition of object wise GLCM mean at lag of 24 pixels (6 m) and angular second moment at lag of 15 pixels (3.75 m), it does not have any improvement in classification.

In this research, the semivariogram parameters, range and sill, have been used for classification. The variogram range measuring texture coarseness is related to the size of the textural features and sill is proportional to the global variance of the textural feature. By comparison of the semivariogram range (refer to Figure 18a) and the radius of the crowns (refer to Figure 16) for each species, one can find that for *Corylus Spp.*, *Alnus Spp.* and *Tilia Spp.* the size of textural features, range, is the same as the size of the crowns. This means that the texture of these species are such a coarse that the textural feature is the crown itself. However for *Plantanus Spp.* the size of textural feature is approximately half of the size of crown. This means that *Plantanus Spp.* forms textural features half of the size of its crown. In this research, the textural feature can be interpreted as the sub-crown. By addition of semivariogram parameters for classification, the accuracy of *Plantanus Spp.* has been decreased since the size of textural features for *Plantanus Spp.* have been confused by the size of *Alnus* and *Tilia Spp.* crowns.



This research shows that the fine structure obtained by subtraction of the Pollock model from the spectral profile reveals more texture compared to the spectral profile itself (refer to Figure 11). Classification based on texture of fine structure instead of texture of spectral profile has improved Kappa coefficient from 0.14 to 0.19. Although classification has been improved, this improvement is not significant and accuracy of classification is still too low. Therefore, texture measurements are not suggested to be considered as a single feature for tree species classification and they should be applied in addition to other features like Pollock parameters to improve classification. This complies with findings of other studies (e.g. Franklin, Maudie, & Lavigne, 2001; Coburn & Roberts, 2004; Y. Zhang, 2001).

In addition, literature review revealed that addition of texture can make modest improvement in classification. It normally improves classification accuracy by 5% to 15% (K. Zhang & Hu, 2012). In this research however, although addition of texture measurements like GLCM texture measures or semi-variogram to Pollock parameters as the additional classification features have improved classification accuracy, this improvement is not significant.

One possible reason could be the choice of texture measurements. In this research, just GLCM texture measurements and semi-variogram have been applied whereas many other texture analysis methods have been developed such as multivariate Gaussian Markov random field (Hazel, 2000), and local binary pattern (Ojala et al., 2002). Finding the reliable texture measurement for tree species classification in urban areas could be a topic for further extensive research.

Another reason for lack of improvement of additional texture measures to the classification can be the choice of classifier. In this research, just Maximum likelihood has been applied for classification and the performance of other classifiers like support vector machine (SVM) has not been explored. Maximum likelihood classifier assumes that each class in each band is normally distributed. In this research most of parameters which were applied for classification, like Pollock parameter  $b$ , are approximately normally distributed. However, some parameter applied for classification are not normally distributed. Maximum likelihood, can also be applied for classification data which are not normally distributed. For non- normally distributed data, one needs to explore the performance of this classifier. Moreover, in maximum likelihood classification the inverse matrix of the covariance becomes unstable in case where there exists very high correlation between two bands. This is the reason why the GLCM texture measures applied for classification have been limited to two measures.

Sample size also influences classification accuracy. Maximum likelihood classification performance depends on reference data. Sufficient reference data should be sampled to allow estimation of mean and covariance matrix of population.

Finally, classification accuracy depends on the differences between the tree species studied for this research. All four tree species (*Plantanus Spp.*, *Corylus Spp.*, *Alnus Spp.*, and *Tilia Spp.*) in the urban study area are deciduous trees. Deciduous trees have similar texture in their tree crown. Most of studies done on classification of tree species, have successfully discriminated deciduous trees from coniferous trees (e.g. Zhang & Hu, 2012).

In this research, by using spectral profile and textural information of tree crowns, *Corylus Spp.* has been classified almost perfectly. However, if one applies the methods introduced in this research for another combination of broad leaves trees, one should not expect to obtain the same results if there are other tree species with crown shapes similar to *Corylus Spp.* However, it is expected that these methods work well enough for separating trees at tree type level (i.e. coniferous and deciduous). In addition, these methods, have been applied on Delft city which mainly has different species of the same genus and large within species

varieties (Chepkochei, 2014). If one applies these methods for another location with another tree species which have less within species variation, one can expect to get more accurate results. Furthermore, once tree species are classified, these method can also be used for extracting more information than species classes like health, age and within species varieties. Moreover, if these methods are applied for another image with coarser resolution, although fine structure information (texture effect) may be lost, coarse structure (spectral profile surface effect) can still be used for classification. In this regard, exploring the effect of scale on the coarse and fine structure of the spectral profile and finding the most appropriate scale for urban tree species classification can be a topic for further studies.



## 7. CONCLUSION AND RECOMMENDATIONS

### 7.1. Conclusion

Coarse structure or low frequency signal component of tree crowns can be described by bell curve models like Pollock, Gaussian and Paraboloid models. RMSE as a goodness of fit showed that the Pollock model with the average RMSE of 0.032 can best approximate the coarse structure of tree crowns for all four species (*Plantanus Spp.*, *Corylus Spp.*, *Alnus Spp.*, and *Tilia Spp.*) compared to Gaussian and Paraboloid models with average RMSE of 0.039 and 0.043 respectively. To describe the coarse structure of the trees of the same species just one model (the Pollock model) is sufficient. In addition, the difference between coarse structure (surface model) of different tree species can be defined by Pollock parameters  $a$ ,  $b$ , and  $n$ . In this regard, *Corylus Spp.* which has the highest values for parameters  $a$  and  $n$  is completely separable from other species. However, *Tilia Spp.* and *Alnus Spp.* which have similar values for parameters  $a$ ,  $b$ , and  $n$  have the lowest separability.

Fine structure or high frequency signal component can be extracted by subtraction of the Pollock model from the spectral profile. In other words, the effects of texture and spectral profile effect can be decomposed by subtraction of the fitted Pollock model from the spectral profile. GLCM texture measurements and semi-variogram have been used for classification of fine structure. Addition of texture information for classification improved Kappa from 0.53 to 0.56 by considering the semivariogram and from 0.53 to 0.55 by considering GLCM texture measurements for classification. However, this improvement is not significant.

Fine structure obtained from subtraction of the Pollock model from the spectral profile revealed more texture compared to the spectral profile itself. Classification based on texture of fine structure instead of texture of spectral profile has improved Kappa coefficient from 0.14 to 0.19. However, this improvement is not significant. *Tilia Spp.* with conditional Kappa 0.41 has the highest accuracy in classification based on only texture of fine structure.

By applying Maximum likelihood classification based on both Pollock parameters and object-wise GLCM texture measurements, *Corylus Spp.* and *Plantanus Spp.* with conditional Kappa of 1.00 and 0.90 respectively classified almost perfectly. *Tilia Spp.* with conditional Kappa of 0.57 classified moderately and *Alnus Spp.* with conditional Kappa of 0.36 classified fairly.

### 7.2. Recommendations

In this research, for texture analysis GLCM texture measurements and semi-variograms have been applied whereas there are many other texture analysis methods. In addition, this research was done on an aerial image with 0.25 m resolution and spectral profile and texture analysis on a different image with different resolution has not been tested. Therefore, further research can be done to find the most reliable texture measurement and scale for tree species classification in urban areas.



## LIST OF REFERENCES

---

- Adler, D., Murdoch, D., & others. (2014). rgl: 3D visualization device system (OpenGL). Retrieved from <http://cran.r-project.org/package=rgl>
- Ardila, J. P. (2012). *Object-based methods for mapping and monitoring of urban trees with multitemporal image analysis*. Published doctoral dissertation, University of Twente Faculty of Geo-Information and Earth Observation (ITC).
- Ardila, J. P., Bijker, W., Tolpekin, V. a., & Stein, A. (2012a). Context-sensitive extraction of tree crown objects in urban areas using VHR satellite images. *International Journal of Applied Earth Observation and Geoinformation*, 15, 57–69. doi:10.1016/j.jag.2011.06.005
- Ardila, J. P., Bijker, W., Tolpekin, V. a., & Stein, A. (2012b). Multitemporal change detection of urban trees using localized region-based active contours in VHR images. *Remote Sensing of Environment*, 124, 413–426. doi:10.1016/j.rse.2012.05.027
- Ardila, J. P., Bijker, W., Tolpekin, V. a., & Stein, A. (2012c). Quantification of crown changes and change uncertainty of trees in an urban environment. *ISPRS Journal of Photogrammetry and Remote Sensing*, 74, 41–55. doi:10.1016/j.isprsjprs.2012.08.007
- Ardila, J. P., Tolpekin, V. a., Bijker, W., & Stein, A. (2011). Markov-random-field-based super-resolution mapping for identification of urban trees in VHR images. *ISPRS Journal of Photogrammetry and Remote Sensing*, 66(6), 762–775. doi:10.1016/j.isprsjprs.2011.08.002
- Barbezat, V., & Jacot, J. (1999). The CLAPA project: Automated classification of forest with aerial photographs. In *International Forum on Automated Interpretation of High Spatial Resolution Digital Imagery for Forestry* (pp. 345–356).
- Blaschke, T. (2004). Object-based contextual image classification built on image segmentation. In *IEEE Workshop on Advances in Techniques for Analysis of Remote Sensed Data* (pp. 113–119).
- Blaschke, T. (2010). Object based image analysis for remote sensing. *ISPRS Journal of Photogrammetry and Remote Sensing*, 65(1), 2–16. doi:10.1016/j.isprsjprs.2009.06.004
- Blaschke, T., & Strobl, J. (2001). What 's wrong with pixels? Some recent developments interfacing remote sensing and GIS. *Interfacign Remote Sensing and GIS*, 14, 12–17.
- Brack, C. L. (2006). Updating urban forest inventories: An example of the DISMUT model. *Urban Forestry & Urban Greening*, 5(4), 189–194. doi:10.1016/j.ufug.2006.09.001
- Brandtberg, T. (2002). Individual tree-based species classification in high spatial resolution aerial images of forests using fuzzy sets. *Fuzzy Sets and Systems*, 132, 371–387.
- Carleer, A., & Wolff, E. (2004). Exploitation of very high resolution satellite data for tree species identification. *Photogrammetric Engineering & Remote Sensing*, 70, 135–140.
- Chepkochei, L. C. (2014). *Urban tree species classification on pixel and object level with worldview-2 image, using maximum likelihood classifier and support vector machine*. University of Twente Faculty of Geo-Information and Earth Observation (ITC).

- Coburn, C. a., & Roberts, a. C. B. (2004). A multiscale texture analysis procedure for improved forest stand classification. *International Journal of Remote Sensing*, 25(20), 4287–4308. doi:10.1080/0143116042000192367
- Dat, M., Mourik, P., & Veen, G. (2006). *Langs bijzondere Delftse bomen (Along special Delft trees)*.
- Dwyer, J. F., Mcpherson, E. G., Schroeder, H. W., & Rowntree, R. A. (1992). Assessing the benefits and costs of the urban forest. *Journal of Arboriculture*, 18(September), 227–234.
- Endress, A. G. (1990). The importance of diversity in selecting trees for urban areas. *Journal of Arboriculture*, 16(June), 143–147.
- Erikson, M. (2004). Species classification of individually segmented tree crowns in high-resolution aerial images using radiometric and morphologic image measures. *Remote Sensing of Environment*, 91(3-4), 469–477. doi:10.1016/j.rse.2004.04.006
- Fournier, R. A., Edwards, G., & Eldridge, N. R. (1995). A Catalogue of potential spatial discriminators for high spatial resolution digital images of individual crowns. *Canadian Journal of Remote Sensing*, 285–298.
- Franklin, S. E., Hall, R. J., Moskal, L. M., Maudie, a. J., & Lavigne, M. B. (2000). Incorporating texture into classification of forest species composition from airborne multispectral images. *International Journal of Remote Sensing*, 21(1), 61–79. doi:10.1080/014311600210993
- Franklin, S. E., Maudie, A. J., & Lavigne, M. B. (2001). Using spatial co-occurrence texture to increase forest structure and species composition classification accuracy. *Photogrammetric Engineering & Remote Sensing*, 67(7), 849–855.
- Franklin, S. E., Wulder, M. a., & Gerylo, G. R. (2001). Texture analysis of IKONOS panchromatic data for Douglas-fir forest age class separability in British Columbia. *International Journal of Remote Sensing*, 22(13), 2627–2632. doi:10.1080/01431160120769
- Gong, P., Sheng, Y., & Blging, G. S. (2002). 3D Model-Based Tree Measurement from High-Resolution Aerial Imagery, 68(11), 1203–1212.
- Gougeon, F. A. (1995a). A Crown-Following approach to the automatic delineation of individual tree crowns in high spatial resolution aerial images. *Canadian Journal of Remote Sensing*, (May 1995).
- Gougeon, F. A. (1995b). Comparison of possible multispectral classification schemes for tree crowns individually delineated on high spatial resolution MEIS Images. *Canadian Journal of Remote Sensing*.
- Gougeon, F. A., & Leckie, D. G. (2003). *Forest information extraction from high spatial resolution images using an individual tree crown approach*. Victoria, BC, Canada.
- Gross, R., & Brajovic, V. (2003). An image preprocessing algorithm for illumination invariant face recognition. In *Audio- and video-based biometric person authentication* (pp. 10–18).
- Hagner, O., & Reese, H. (2007). A method for calibrated maximum likelihood classification of forest types. *Remote Sensing of Environment*, 110(4), 438–444. doi:10.1016/j.rse.2006.08.017
- Hájek, F. (2006). Object-oriented classification of Ikonos satellite data for the identification of tree species composition. *Journal of Forest Science*, (4), 181–187.

- Haralick, R. M., Shanmugam, K., & Dinstein, I. (1973). Textural features for image classification. *IEEE Transactions on Systems, Man and Cybernetics*, 3, 610–620.
- Hay, G. J., & Castilla, G. (2008). Geographic object-based image analysis ( GEOBIA ): A new name for a new discipline. In T. Blaschke, S. Lang, & G. J. Hay (Eds.), *Lecture notes in geoinformation and cartography* (pp. 75–89). Berlin: Springer.
- Hazel, C. G. (2000). Multivariate Gaussian MRF for multispectral scene segmentation and anomaly detection. *IEEE Transactions on Geoscience and Remote Sensing*.
- Hirschmugl, M., Ofner, M., Raggam, J., & Schardt, M. (2007). Single tree detection in very high resolution remote sensing data. *Remote Sensing of Environment*, 110(4), 533–544. doi:10.1016/j.rse.2007.02.029
- Horn, H. S. (1971). *The adaptive geometry of trees* (p. 144). Princeton University Press.
- Jakomulska, A., & Clarke, K. C. (2000). Variogram-derived measures of textural image classification. In *Proceedings of the Third European Conference on Geostatistics for Environmental Applications* (pp. 345–355).
- Key, T., Warner, T. A., McGraw, J. B., & Fajvan, M. A. (2001). A Comparison of multispectral and multitemporal information in high spatial resolution imagery for classification of individual tree species in a temperate hardwood forest. *Remote Sensing of Environment*, 100–112.
- Kim, C., & Hong, S.-H. (2008). Identification of tree species from high resolution satellite imagery by using crown parameters. In C. M. U. Neale, M. Owe, & G. D'Urso (Eds.), *Proceeding of Remote Sensing for Agriculture, Ecosystems, and Hydrology* (Vol. 7104, p. 71040N–71040N–8). doi:10.1117/12.800074
- Landis, R., & Koch, G. (1977). The measurement of observer agreement for categorical data. *Biometrics*, 33.
- Larsen, M., & Rudemo, M. (1997). Using ray – traced templates to find individual trees in aerial photographs. In *Proceeding of the 10th Scandinavian Conference on Image Analysis* (pp. 1007–1014).
- Leckie, D. (2003). Stand delineation and composition estimation using semi-automated individual tree crown analysis. *Remote Sensing of Environment*, 85(3), 355–369. doi:10.1016/S0034-4257(03)00013-0
- Lucieer, A. (2004). *Uncertainties in segmentation and their visualisation*. Published doctoral dissertation, University of Twente Faculty of Geo-Information and Earth Observation (ITC).
- Mayer, H., Bacher, U., & Ebner, H. (1999). Automatic extraction of trees from aerial imagery. In *Proceedings, Workshop on Semantic modeling for the acquisition of topographic information from images and maps (SMATT'99)* (pp. 155–165).
- Meyera, P., Staenzb, K., & Ittena, K. I. (1996). Semi-automated procedures for tree species identification in high spatial resolution data from digitized colour infrared-aerial photography. *ISPRS Journal of Photogrammetry and Remote Sensing*, 51(1), 5–16. doi:10.1016/0924-2716(96)00003-2
- Mora, B., Wulder, M. a., & White, J. C. (2010). Identifying leading species using tree crown metrics derived from very high spatial resolution imagery in a boreal forest environment. *Canadian Journal of Remote Sensing*, 36(4), 332–344. doi:10.5589/m10-052
- Moskal, L. M., Styers, D. M., & Halabisky, M. (2011). Monitoring urban tree cover using object-based image analysis and public domain remotely sensed data. *Remote Sensing*, 3(12), 2243–2262. doi:10.3390/rs3102243



- Ojala, T., Pietikainen, M., & Maenpaa, T. (2002). Multiresolution gray-scale and rotation invariant texture classification with local binary patterns. *IEEE Transactions on Pattern Analysis and Machine Intelligence*, 24(7), 971–987.
- Pollock, J. (1996). *The automatic recognition of individual trees in aerial images of forests based on a synthetic tree crown image model*. Published doctoral dissertation, University of British Columbia.
- Pollock, R. J. (1994). A model-based approach to automatically locate tree crowns in high spatial resolution images. In *Image and Signal Processing for Remote Sensing* (Vol. 2315, pp. 526–537). SPIE.
- Pouliot, D., King, D., Bell, F., & Pitt, D. (2002). Automated tree crown detection and delineation in high-resolution digital camera imagery of coniferous forest regeneration. *Remote Sensing of Environment*, 82(2–3), 322–334. doi:10.1016/S0034-4257(02)00050-0
- Pu, R., & Landry, S. (2012). A comparative analysis of high spatial resolution IKONOS and WorldView-2 imagery for mapping urban tree species. *Remote Sensing of Environment*, 124, 516–533. doi:10.1016/j.rse.2012.06.011
- Roller, B. N. (2000). Intermediate multispectral satellite sensors. *Journal of Forestry*, 6(June), 32–35.
- Russell, C., & Kass, G. (1999). *Assessing the accuracy of remotely sensed data: principles and practices* (p. 137).
- Ryer, A. (1998). *Light measurement handbook* (p. 64).
- Straub, B., & Heipke, C. (2001). Automatic extraction of trees for 3D-city models from images and height data, (1999), 267–277.
- Sugumaran, R., Pavuluri, M. K., & Zerr, D. (2003). The use of high-resolution imagery for identification of urban climax forest species using traditional and rule based classification approaches, 41(9), 1933–1939.
- Teillet, P. M., Guindon, B., & Goodenough, D. G. (1982). On the slope-aspect correction of multispectral scanner data. *Canadian Journal of Remote Sensing*, 8(2), 84–106. doi:10.1080/07038992.1982.10855028
- Thomas, N., Hendrix, C., & Congalton, R. G. (2003). A comparison of urban mapping methods using high-resolution digital imagery. *Photogrammetric Engineering & Remote Sensing*, 69(9), 963–972. doi:10.14358/PERS.69.9.963
- Turner, S., Slater, D., & Ennos, A. R. (2012). Failure of forks in clonal varieties of *Platanus x acerifolia*. *Arboricultural Journal*, 34(4), 179–189.
- USDA. (2002). *Community tree inventory: Data collection. Technical Report*.
- Warner, T. A., Lee, J. Y., & McGraw, J. B. (1998). Delineation and identification of individual trees in the eastern deciduous forest. In *Automated Interpretation of High Spatial Resolution Digital Imagery for Forestry* (pp. 81–91). Victoria, British Columbia, Canada.
- Webster, R., & Oliver, M. (2008). *Geostatistics for environmental scientists* (p. 332).
- White, J. D., Kroh, G. C., & Pinder, J. E. (1995). Forest mapping at Lassen volcanic national park, California, using Landsat TM data and a geographical information system. *Photogrammetric Engineering and Remote Sensing*, 61(3), 299–305.

- Wolf (né Straub), B.-M., & Heipke, C. (2007). Automatic extraction and delineation of single trees from remote sensing data. *Machine Vision and Applications*, 18(5), 317–330. doi:10.1007/s00138-006-0064-9
- Wolf, K. L. (2004). Economics and public value of urban forests. *Urban Agriculture Magazine*, 13(December), 31–33.
- Wulder, M. a., Hall, R. J., Coops, N. C., & Franklin, S. E. (2004). High spatial resolution remotely sensed data for ecosystem characterization. *BioScience*, 54(6), 511. doi:10.1641/0006-3568(2004)054[0511:HSRRSD]2.0.CO;2
- Zhang, K., & Hu, B. (2012). Individual urban tree species classification using very high spatial resolution airborne multi-spectral imagery using longitudinal profiles. *Remote Sensing*, 4(12), 1741–1757. doi:10.3390/rs4061741
- Zhang, W., Hu, B., Jing, L., Woods, M. E., & Courville, P. (2008). Automatic forest species classification using combined LIDAR data and optical imagery. In *Proceeding of the International Geoscience and Remote Sensing Symposium* (pp. 134–137).
- Zhang, Y. (2001). Texture-integrated classification of urban treed areas in high-resolution color-infrared imagery. *Photogrammetric Engineering & Remote Sensing*, 67(December), 1359–1365.